Year XXXI Nº 43 December 2023

UNDERGROUND MINING ENGINEERING

Podzemni radovi

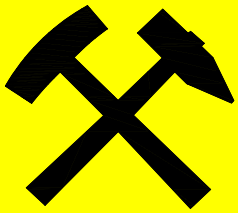

University of Belgrade – Faculty of Mining and Geology

UDK 62

ISSN 0354-2904
eISSN 2560-3337

UNDERGROUND MINING ENGINEERING

PODZEMNI RADOVI

N°43

http://ume.rgf.bg.ac.rs
e-mail: editor.ume@rgf.bg.ac.rs

Belgrade, December 2023.

UNDERGROUND MINING ENGINEERING 43 (2023) UDK 62
UNIVERSITY OF BELGRADE - FACULTY OF MINING AND GEOLOGY ISSN 03542904

UNDERGROUND MINING ENGINEERING - PODZEMNI RADOVI

Publishing supported by: University of Belgrade – Faculty of Mining and Geology, Mining Section

Publisher: University of Belgrade - Faculty of Mining and Geology

For publisher: D.Sc. Biljana Abolmasov, Dean of Faculty of Mining and Geology

Printed by: SaTCIP, Vrnjačka Banja

Circulation: 200 copies

The first issue of the journal "Podzemni radovi" (Underground Mining Engineering) was published back in 1982. Its founders were: Business Association Rudis - Trbovlje and the Faculty of Mining and Geology Belgrade. After publishing only four issues, however, the publication of the journal ceased in the same year.

Ten years later, in 1992, on the initiative of the Chair for the Construction of Underground Roadways, the Faculty of mining and Geology as the publisher, has launched journal "Podzemni radovi". The initial concept of the journal was, primarily, to enable that experts in the field of underground works and disciplines directly connected with those activities get information and present their experiences and suggestions for solution of various problems in this scientific field.

Development of science and technique requires even larger multi-disciplinarity of underground works, but also of the entire mining as industrial sector as well. This has also determined the change in editorial policy of the journal. Today, papers in all fields of mining are published in the "Underground Mining Engineering", fields that are not so strictly in connection with underground works, such as: surface mining, mine surveying, mineral processing, mining machinery, environmental protection and safety at work, oil and gas engineering and many others.

Extended themes covered by this journal have resulted in higher quality of published papers, which have considerably added to the mining theory and practice in Serbia, and which were very useful reading material for technical and scientific community.

A wish of editors is to extend themes being published in the "Underground Mining Engineering" even more and to include papers in the field of geology and other geo-sciences, but also in the field of other scientific and technical disciplines having direct or indirect application in mining.

The journal "Underground Mining Engineering" is published twice a year, in English language. Papers are subject to review.

This information represents the invitation for cooperation to all of those who have the need to publish their scientific, technical or research results in the field of mining, but also in the field of geology and other related scientific and technical disciplines having their application in mining.

Editors

UNDERGROUND MINING ENGINEERING 43 (2023) UDK 62
UNIVERSITY OF BELGRADE - FACULTY OF MINING AND GEOLOGY ISSN 03542904

TABLE OF CONTENTS

UNDERGROUND MINING ENGINEERING 43 (2023) 1-16 UDK 62
UNIVERSITY OF BELGRADE - FACULTY OF MINING AND GEOLOGY ISSN 03542904

Original scientific paper

DIFFERENT APPROACH TO SURFACTANT SCREENING METHODS FOR ASP FLOODING

Darko Popić[1], Jasna Pantić[1], Milos Tripković[1], Bojan Martinović[1], Andrej Antropov[1], Miroslav Crnogorac[2]

Received: July 21, 2023 **Accepted:** August 5, 2023

Abstract:

Selection of adequate surfactant is one of the most important steps in preparation for ASP EOR. There are many parameters to be taken in considerations in this process but different authors are prioritizing different parameters. Shown here is comparative analysis of two surfactants chosen according difference set of priorities, in one low IFT and stability and type of created microemulsion was priority (Surfactant A) and in another mobility of created microemulsion (Surfactant B). Bottle test was done with both surfactants to assess the stability of microemulsion at formation temperature, and coreflood test to assess ability of surfactant to mobilize trapped oil. During first round of tests Surfactant A gave better results, very low IFT and stabile Windsor type III microemulsion while Surfactant B gave higher IFT and Windsor type I microemulsion. During coreflood test Surfactant B performed better in terms of oil recovery factor (ORF) and injection pressures. Apparently, stabile Windsor type III microemulsion that is considered desirable in ASP injection and widely prioritized in surfactant selection process can cause decrease in permeability and injectivity issues. Good results can be obtained with IFT in "moderately" low range and stability of microemulsion is not critical in terms of oil recovery factor.

Keywords: Chemical EOR; Surfactant selection; Ultra low IFT; Coreflood testing

1 INTRODUCTION

Being that primary and secondary methods of oil production can extract only limited part of original oil in place (OOIP), and with most of the big oilfields being in late phase of production, there is higher demand to increase oil recovery from oilfields already in production. Conventional oil production methods leave large amounts of oil in reservoir, so there is a need for cost efficient methods to boost production. This goal is achieved by chemical enhanced oil recovery (cEOR) methods – injecting alkali, surfactant and

[1] NTC NIS Naftagas doo, Narodnog fronta 12, 21000 Novi Sad
[2] University of Belgrade - Faculty of Mining and Geology, Đušina 7, 11000 Belgrade
E-mails: darko.popic@nis.rs; jasna.pantic@nis.rs; milos.tripkovic@nis.rs: bojan.martinovic@nis.rs: antropov.av@nis.rs; miroslav.crnogorac@rgf.bg.ac.rs

polymer separately or in mixture (ASP) in to reservoir to mobilize oil that couldn't be extracted by conventional production methods.

Chemical EOR / ASP methods are studied and implemented for decades in various condition all over the world. In this period significant progress was made in terms of developing products that can be used in harsh reservoir conditions (heavy oil, high temperature and salinity) but overall principle stayed the same. Alkali is reacting with organic acids that are occurring in oil naturally to form soap (Gao et al., 1995; Mahdavi & Zebarjad, 2018). This newly formed soap together with injected surfactant have a task to decrease interphase tension (IFT) between water and oil, change wettability of porous environment and create mobile microemulsion that will be produced with help of viscous polymer front arriving after surfactant (Mohyaldinn et al., 2019; Wang et al., 2007).

Surfactants are surface-active substances with polar (or hydrophilic) head and a nonpolar (hydrophobic) tail, this allows them to have affinity to aqueous and non-aqueous phase due to the amphiphilic nature. Generally speaking all surfactant types can reduce the IFT between the aqueous and oil phase and change environment wettability to more water-wet conditions, but selecting the suitable type of surfactant is very crucial in terms of solubility, thermal and chemical stability, and adsorption of the surfactant under harsh reservoir conditions (Borchardt et al., 1985; Eftekhari et al., 2015). Generally, surfactants are classified into main four groups: anionic, cationic, and non-ionic and zwitterionic (also known as amphoteric) (Gupta et al., 2020; Mahboob et al., 2022; Bera & Mandal, 2015).

The key to successful cEOR is selecting right surfactant or alkali surfactant mixture that will effectively mobilize trapped oil held in small pores by capillary forces. It is achieved through decrease of IFT to a point of forming microemulsion and changing reservoir rock wettability. In surfactant selection process one of the main criteria is type of microemulsion formed with oil and its stability (Bera & Mandal, 2015; Guo et al., 2012; Salager et al., 2013) – Windsor type III microemulsion that is stabile in time at reservoir condition. Some authors suggest that most important criteria is mobility of formed microemulsion (Puskas et al., 2017, 2018). Stabile Windsor type III emulsion can be achieved only with very low IFT values (order of 10-3 mN/m or lower) but mobile microemulsion can be achieved with higher IFT values (order of 10-2 mN/m).

In this paper are presented two different surfactants chosen by these two criteria for same reservoir, using two mentioned principles. Since different guiding principles were used in these two cases it was impossible to compare these surfactants except to test their performance with bottle test, emulsion stability and core flood experiments.

All experiments mentioned in this paper were done as a part of preparation for chemical EOR project on oilfield in northern part of Serbia. Reservoir rock is upper Miocene sandstone, medium to coarse grained, carbonaceous in parts, loose to moderately well

cemented with siliceous and calcareous cement. Entire reservoir is generally high permeable, with permeability ranging from 1 to 6 Darcy.

2 METHODS AND MATERIALS

Reservoir conditions and oil characteristics, main criteria for surfactant selection, were shared with surfactant manufacturers. Of all samples received, the two most promising were selected: 1st for its low IFT value and 2nd for high oil displacement efficiency determined by thin layer chromatography. For both surfactants optimal concentration is set to 0,5%. Characteristics of tested surfactants are shown in table 1.

Table 1 Main characteristics of surfactants used in experiments

Product name	Composition	Measured IFT	pH of aqueous solution
Surfactant A	mixture of mono and diesters of phosphoric acid and ethoxylated C12-C15 alcohols with isobutanol	IFT: 1,9-2,1*10^{-4} mN/m (in 0,5% solution)	5,93
Surfactant B	Sulfonic acid derivative and fatty acid methylester derivative in 2-butoxyethanol solvent	IFT: 0,0078 mN/m (in 0,5% solution)	7,5 - 9,5

Reservoir oil has total acid number (TAN) ranging from 0,7 - 2,0 mg KOH/g usage of alkalis is recommended (Sheng, 2015; Chang et al., 2006). Surfactant A has a low pH value so it is combined with 1% of Na_2CO_3 to boost oil displacement. Addition of alkali will boost oil displacement through saponification process that occurs when alkali comes in in contact with naphthenic acids in oil (Gbadamosi et al., 2019), and also to decrease adsorption of surfactant to rock surface (Zhong et al., 2020). Surfactant B has pH around 8,5 so adding alkali in mixture wouldn't increase efficiency of oil displacement – what was the intention of manufacturer.

Since salinity and TDS of formation water is not high (11 g/l of NaCl equivalent and 13,9 g/l TDS) and very low iron content (below 2 mg/l) it was decided that formation water separated at gathering station will be used for preparation of ASP / SP mixture during field operations. For purpose of laboratory testing all ASP/SP mixtures were prepared with modelled formation water, recipe is shown in table 2.

Table 2 Salts used to prepare Main characteristics of surfactants used in experiments

Salts	concentration (g/l)
$CaCl_2$	0,20
$MgCl_2 \times 6H_2O$	0,10
Na_2SO_4	0,05
$NaHCO_3$	5,10
NaCl	7,50

2.1 Bottle test

With both surfactants bottle test was performed to assess and compare ability to form microemulsion, quantity and stability of microemulsion. Bottle test was performed with reservoir oil, extracted from produced fluid only by heating without chemicals and with surfactant and alkali/surfactant mixture prepared with modelled formation water. Oil and alkali surfactant / surfactant solution were mixed in 1:1 ratio. After turning the bottle upside down continuously by hand for 2 minutes, samples were placed into a thermo regulated oven at 67°C (formation temperature) for a period of 30 and 23 days, respectively. Samples were taken out once per day to check for presence, type and quantity of microemulsion.

Results of bottle test with mixture 0,5% Surfactant A + 1% Na2CO3 and 0,5% Surfactant B are shown in figures 1 and 2.

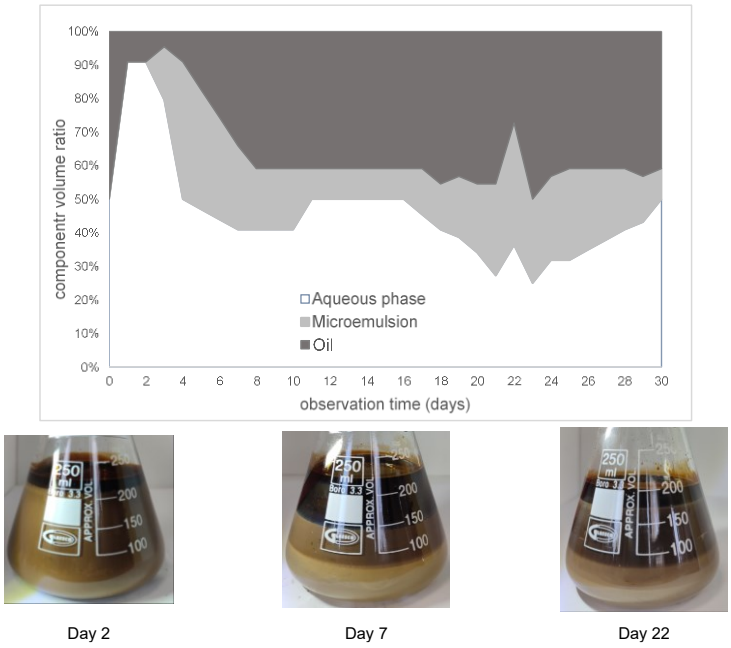

Figure 1 Microemulsion stability during bottle test with Surfactant A. (a) day 2: Windsor type I microemulsion; (b) day 7: Windsor type III microemulsion, (c) day 22: Windsor type III microemulsion

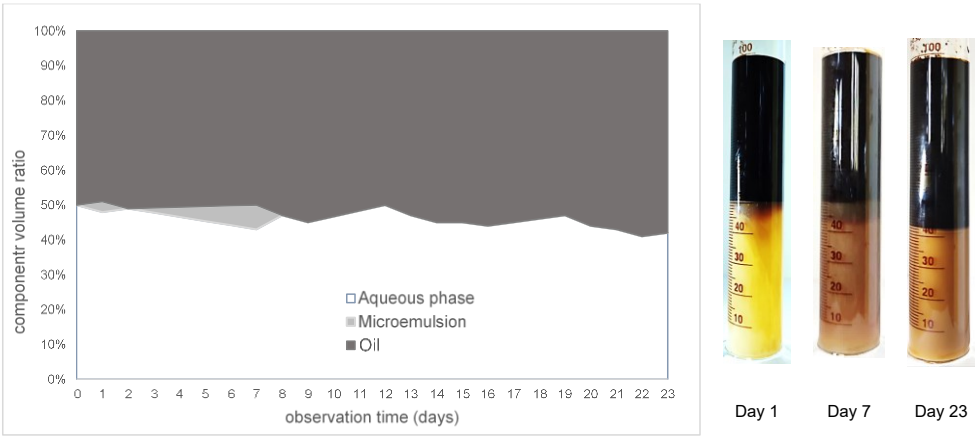

Figure 2 Microemulsion stability during bottle test with Surfactant B. (a) day 1: day 1: Windsor type III microemulsion, (b) day 7: Windsor type III / type I microemulsion; (c) day 23: Windsor type I microemulsion

With both surfactants bottle test was performed to assess and compare ability to form microemulsion, quantity and stability of microemulsion. Bottle test was performed with reservoir oil, extracted from produced fluid only by heating without chemicals and with surfactant and alkali/surfactant mixture prepared with modelled formation water. Oil and alkali surfactant / surfactant solution were mixed in 1:1 ratio. After turning the bottle upside down continuously by hand for 2 minutes, samples were placed into a thermo regulated oven at 67°C (formation temperature) for a period of 30 and 23 days, respectively. Samples were taken out once per day to check for presence, type and quantity of microemulsion.

With Surfactant A Windsor type I microemulsion was formed immediately after mixing when 80% of present oil was dispersed in water phase. Gradually, after 2 days Windsor type I microemulsion is starting to break apart with increase in free oil phase and forming of type III microemulsion. Aqueous phase is not clear, it contains lots of dispersed oil and it looks like aqueous phase in Windsor type I microemulsion. Microemulsion layer formed between aqueous and oil phase is relative stabile and, with changes in volume, it exists during entire observation period of 30 days. With Surfactant B immediately after mixing small quantity of Windsor type III microemulsion is formed, with oil phase dispersed in aqueous phase so it resembles type I microemulsion. Windsor type III microemulsion is stabile for 7 days and it is dispersed. After that mixture resembles Windsor type I microemulsion with oil in water emulsion but volume of oil phase is slowly increasing over observation period so part of water is dispersed in oil phase as well.

2.2 Coreflood test

To test ability of these surfactants to mobilize residual oil from porous rock sample coreflood tests were performed with ASP / SP mixtures prepared with Surfactant A (ASP mixture) and Surfactant B (SP mixture). As criteria to determine surfactant performance changes in oil recovery factor (ORF) were used. ORF represent decrease in residual oil saturation (Soi-Sor) divided by initial oil saturation (Soi). Test were performed on cylindrical samples formed from sand and poorly consolidated sandstone retrieved during coring operations. All rock samples undergo soxhlet extraction using toluene to remove any residual oil or contamination. After extraction sand was tightly packed in thermoresistant sleeves to form cylindrical samples 3,81cm (1,5 inch) in diameter and approximately 13,5 cm (5,3 inch) long. Sample characteristics are shown in table 3.

For preparation of ASP mixture (in case of Surfactant A) and SP mixture (Surfactant B) as polymer was used HPAM with high molecular weight (18-20 106 Da) in concentration sufficient to reach target mixture viscosity of 10 mPa*s that was chosen according to oil viscosity and average reservoir permeability. As alkali 1% of Na2CO3 was used. All mixtures were prepared with model formation water. For purpose of experiment reservoir oil, extracted from produced fluid only by heating without chemicals, was diluted with petroleum benzine (C7 n and iso alkanes with cyclic HC) to decrease its

viscosity to value at reservoir conditions. During experiment, two ASP/SP mixtures were used: first with surfactant concentration of 0,1% and second of 0,5% - to imitate dilution effect that will happen in reservoir.

Coreflood experiments were performed on "in house" coreflood system, with coreholder placed in thermo-regulated oven, with regulation of back-pressure (pore pressure), lateral pressure (overburdon) and syringe pump for fluid injection. Setup of coreflood system is shown on figure 3. Coreflood test were performed at 67 °C reservoir temperature, with 140 Bar of overburdon pressure and with 65 Bar of pore pressure (back pressure).

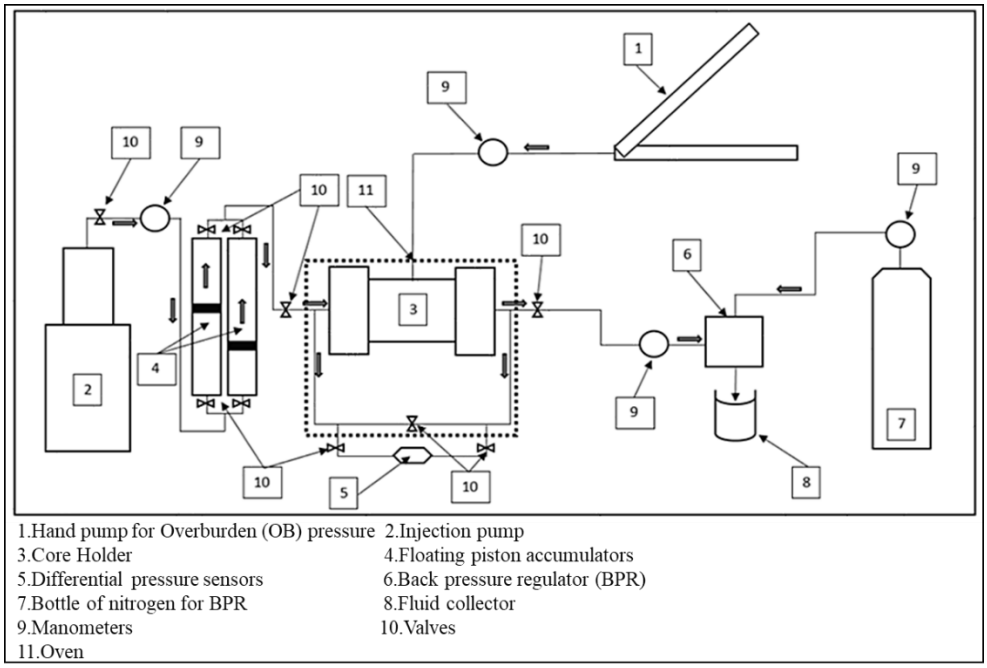

Figure 3 Setup of coreflood system used in experiments

Coreflood experiment was done in as per following steps:

- Injecting the model formation water (MFW) at three flow rates until the differential pressure stabilizes (minimum 1 pore volume), goal is to determine linear permeability for MFW (Kw).

- Injection of oil at a constant flow rate until the differential pressure stabilizes (minimum 3 pore volumes). Fluid at outlet is sampled and initial water saturation (Swi) is determined by measuring quantity of produced fluid.

- Partial isolation of the core sample on reservoir conditions (aging process) for a period of 72 h. Oil is periodically injected for six hours at a lowest possible flow rate.

- Oil injection at three flow rates until the differential pressure stabilizes (minimum 1 pore volume). Linear effective permeability for oil (Ko@Swi) is determined.

- Injecting MFW at constant flow rate until the differential pressure stabilizes (minimum 3 pore volumes). During injection, fluid at outlet is continuously sampled, the volume of displaced oil is monitored to determine change in oil recovery factor (ORF1). After stabilizing the differential pressure, the effective permeability for MFW (Kw1@Sor) is determined. 2-3 pore volumes of MFW re injected at an increased flow rate to confirm ORF value.

- Injecting first ASP / SP composition (alkali + polymer + 0.1% surfactant concentration), total of 2 pore volumes at constant flow rate. Differential pressure is recorded and the fluid at the outlet is continuously sampled (every 0.2 pore volume). Volume of displaced oil is monitored to determine change in oil recovery factor (ORF2).

- Injecting second ASP / SP composition (alkali + polymer + 0.5% surfactant concentration), total of 2 pore volumes at constant flow rate. Differential pressure is recorded and the fluid at the outlet is continuously sampled (every 0.2 pore volume). Volume of displaced oil is monitored to determine change in oil recovery factor (ORF3).

- Injecting MFW at constant flow rate. The MFW is pressed until the differential pressure stabilizes (minimum 3 pore volumes). During indentation, the fluid at the outlet is continuously sampled every 0.5 pore volume Volume of displaced oil is monitored to determine change in oil recovery factor (ORF4). After differential pressure is stabilized, the effective permeability for MFW (Kw2@Sor) is determined.

Results of coreflood experiments were shown in figures 4 and 5 and in table 3. Amount of oil produced during coreflood test is expressed through Oil Recovery Factor (ORF): ratio between decrease in oil saturation of certain phase and initial oil saturation.

Changes in differential pressure during injections are also shown on figures 4 and 5 as indicators in changes in permeabilities during and after ASP / SP mixture injections: Resistivity modification and residual resistivity factor. Resistance modification (Rm) (Ferreira & Moreno, 2019; Thomas, 2019) is calculated from differential pressure during water injection prior to ASP/SP injection and differential pressure during ASP/SP injection at same flow rate using equation 1.

$$Rm = \frac{\Delta P_p}{\Delta P_w{}^{\text{before}}} \quad (1)$$

ΔP_p Differential pressure during ASP/SP injection

$\Delta P_w{}^{\text{before}}$ Differential pressure during water injection before ASP/SP mixture

Residual resistance factor (RFF) (Ferreira & Moreno, 2019; Thomas, 2019) is calculated from differential pressure during water injection before and after ASP/SP mixture is injected through the sample using equation 2.

$$RRF = \frac{\Delta P_w{}^{\text{after}}}{\Delta P_w{}^{\text{before}}} \quad (2)$$

$\Delta P_w{}^{\text{after}}$ Differential pressure during water injection after ASP/SP mixture

$\Delta P_w{}^{\text{before}}$ Differential pressure during water injection before ASP/SP mixture

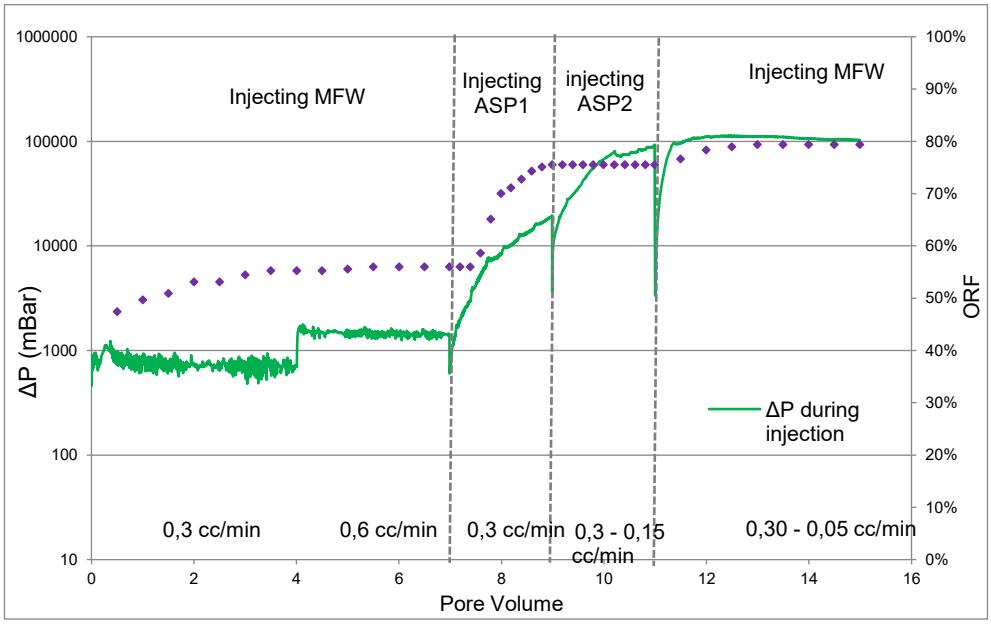

Figure 4 Changes in differential pressure and ORF during injection of ASP mixtures prepared with Surfactant A. ASP1 – mixture prepared with 0,1% surfactant concentration, ASP2 – mixture prepared with 0,5% surfactant concentration

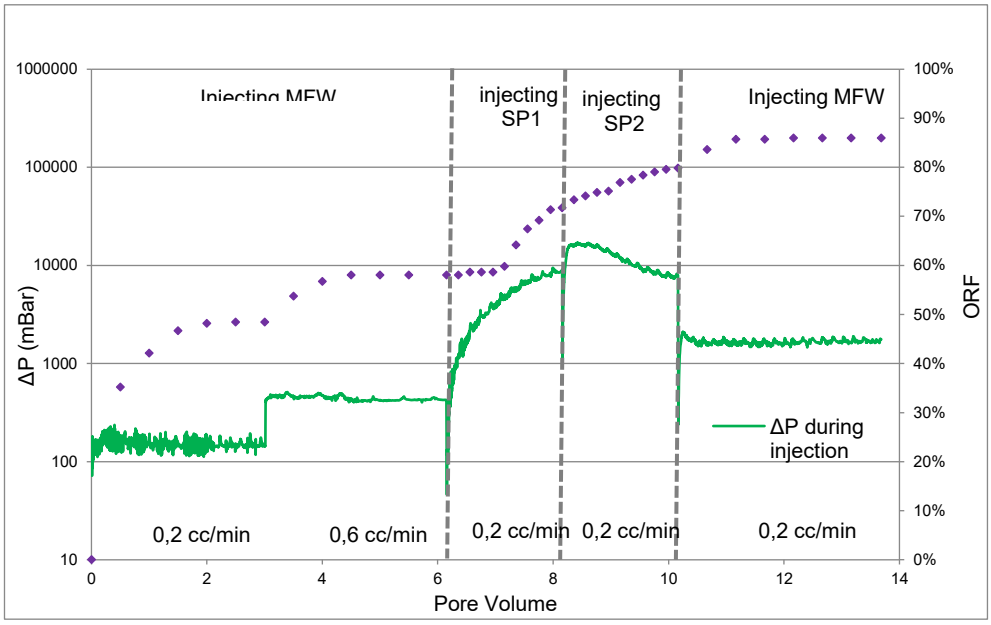

Figure 5 Changes in differential pressure and ORF during injection of SP mixtures prepared with Surfactant B. SP1 – mixture prepared with 0,1% surfactant concentration, SP2 – mixture prepared with 0,5% surfactant concentration

Table 3 Results obtained during coreflood tests with both surfactants, both tests performed in same way on similar samples.

Phase	Surfactant A		Surfactant B	
	Results	Calculated values	Results	Calculated values
Core sample characteristics	Length: 14,575 cm Porosity: 30,21% Pore volume: 44,94 ml Kw: 182,29 mD		Length: 13,705 cm Porosity: 32,7% Pore volume: 49,73 ml Kw: 165,64 mD	
Injecting oil / reaching Soi	ORF = 0 %		ORF = 0 %	
Injecting MFW (6 PV) to reach Sor	ORF1 = 56,25% Kw1@Sor = 13,64 mD		ORF1 = 58,05% Kw1@Sor = 12,24 mD	
Injecting first ASP / SP composition (2 PV)	1% Na_2CO_3 0,1% Surfactant A 0,1% Polymer	Rm1 = 85,83	0,1% Surfactant B 0,1% Polymer	Rm1 = 62,52
Injecting second ASP / SP composition (2 PV)	ORF2 = 75,53 % 1% Na_2CO_3 0,5% Surfactant A 0,1% Polymer	Rm2 = 816,4	ORF2 = 71,72 % 0,5% Surfactant B 0,1% Polymer	Rm2 = 53,69
Injecting MFW (2 PV)	ORF3 = 75,53 % ORF4 = 79,38 % Kw2@Sor = 0,005 mD	RRF = 2718,3	ORF3 = 79,84 % ORF4 = 85,92 % Kw2@Sor = 1,046 mD	RRF = 12,04

3 RESULTS

3.1 Bottle test results

Tested surfactants react differently with oil. Surfactant A in combination with alkali (Na2CO3) is decreasing IFT to a value low enough to allow forming of stabile Windsor type III microemulsion, this kind of microemulsion is desirable in chemical EOR (Ahmed & Elraies, 2018) because it better mobilize trapped oil. After initial mixing, it took 2 days for Windsor type III microemulsion to form but it was stabile without mixing for 28 days after that. Surfactant B is forming Windsor type I microemulsion, oil is dispersed in water phase with smaller part of water dispersed in oil phase as well. Clearly, IFT is significantly reduced to allow mixing oil and water but not enough to allow forming of stabile Windsor type III microemulsion. Certain quantity of Windsor type III microemulsion formed after mixing but until 7-8 days it all disappeared.

If only criteria of quantity, stability, and type of microemulsion is taken in account, Surfactant A is giving much better results. With Surfactant B, Windsor type III microemulsion is present only in short period after mixing but mixing process is taking place is porous environment in reservoir during ASP/SP mixture injection (Bob, 2016; Villermaux, 2012). Because of that stability of microemulsion cannot be considered as excluding criteria in surfactant selection process.

3.2 Coreflood test results

If we compare results of coreflood tests by oil recovery factor (ORF) value it is visible that both surfactants are able to mobilize big part of oil trapped after water sweep, with Surfactant B performing slightly better in overall results (A with ORF 79%, B with ORF 85%). From that perspective it looks like that type and quantity of microemulsion formed is not excluding criteria when it comes to surfactant selection – Surfactant B during bottle test formed very small amount of Windsor type III microemulsion, while most of the water phase looked like type I microemulsion.

From the curve shown on figure 4 it is visible that Surfactant A is mobilizing residual oil immediately after injection, even in 0,1% concentration. With increase in surfactant concentration there is no increase in oil production and there is just slight increase in oil production in post flush phase when water is injected through the sample. From Surfactant B performance, shown on figure 5, it is visible that mobilization of residual oil is not that fast and that efficient in low concentration as with Surfactant A. With increase in surfactant concentration ORF is increasing as well and there is moderate increase in oil recovery during post flush period. For both surfactants speed of reaction to surfactant and oil recovery during post flush stage is happening because of adsorption / desorption process during different stages of coreflood experiment (Gogoi, 2011; Liu et al., 2004). Significant difference between this two coreflood experiments is in differential pressure during injection stages. With Surfactant A there is big increase in

differential pressure during transitioning from lower to higher surfactant concentration and no pressure decrease during post flush phase. With Surfactant B there is a slight pressure increase when mixture with higher surfactant concentration is injected and there is pressure drop during post flush phase when water is injected. This is clearly visible in changes in Resistance modification (Rm) and Residual resistance factor (RFF) values shown in table 3. This difference in injection pressures between two coreflood experiments cannot be caused by polymer retention since the same polymer is used in same concentration on very similar rock sample in both experiments.

4 CONCLUSION

It seems that difference in injection pressures between two coreflood experiments is caused by significant quantity of stabile Windsor type III microemulsion because only difference between experiments is surfactant used and its way of interaction with oil. Stabile microemulsions can have high viscosity and cause flow restriction that can cause injection problems, especially with single surfactant system.

- From performance of Surfactant B, it is visible that absence of stabile Windsor type III microemulsion is not disadvantage during chemical EOR operations.

- Even with IFT value in “moderately” low range, good results on terms of ORF value can be obtained.

- Initial screening criteria that IFT value for oil / surfactant solution has to be as low as possible and that microemulsion has to be stabile Windsor type III is not valid.

- With surfactant that decrease IFT to “moderately” low value there is less risk that highly viscous microemulsions will form and cause flow problems in reservoir.

- If microemulsions are only stabile during, and shortly after mixing, there is less chance that chemical EOR operations can cause problems during oil preparation process in gathering stations, after oil is produced. If oil with traces of surfactant reaches production wells it is better that microemulsion lose stability immediately after “mixing” in porous environment stops and starts to dissolve to separate phases: oil and formation water. In this way impact on produced fluid is minimized.

REFERENCES

AHMED, S., & ELRAIES, K. A. (2018) Microemulsion in Enhanced Oil Recovery. In *InTech eBooks*. https://doi.org/10.5772/intechopen.75778

BERA, A., & MANDAL, A. (2015) Microemulsions: a novel approach to enhanced oil recovery: a review. *Journal of Petroleum Exploration and Production Technology*, *5*(3), 255–268. https://doi.org/10.1007/s13202-014-0139-5

BOB, B. (2016, October 25) *Mixing of Fluid by Dispersion | Fundamentals of Fluid Flow in Porous Media*. Special Core Analysis & EOR Laboratory | PERM Inc. https://perminc.com/resources/fundamentals-of-fluid-flow-in-porous-media/chapter-5-miscible-displacement/fluid-properties-miscible-displacement/macroscopic-displacement-efficiency/mixing-fluid-dispersion/

BORCHARDT, J., BRIGHT, D. B., DICKSON, M., & WELLINGTON, S. (1985) Surfactants for CO2 Foam Flooding. In *All Days*. https://doi.org/10.2118/14394-ms

CHANG, H., ZHANG, Z. P., WANG, Q., XU, Z., GUO, Z. J., SUN, H., CAO, X., & QIAO, Q. (2006) Advances in Polymer Flooding and Alkaline/Surfactant/Polymer Processes as Developed and Applied in the People's Republic of China. *Journal of Petroleum Technology*, *58*(02), 84–89. https://doi.org/10.2118/89175-jpt

EFTEKHARI, A., KRASTEV, R., & FARAJZADEH, R. (2015) foam stabilized by fly Ash Nanoparticles for Enhancing Oil Recovery. *Industrial & Engineering Chemistry Research*, *54*(50), 12482–12491. https://doi.org/10.1021/acs.iecr.5b03955

FERREIRA, V. H. S., & MORENO, R. B. Z. L. (2019) Rheology-based method for calculating polymer inaccessible pore volume in core flooding experiments. *E3S Web of Conferences*, *89*, 04001. https://doi.org/10.1051/e3sconf/20198904001

GAO, S., LI, H., & LI, H. (1995) Laboratory Investigation of Combination of Alkali/Surfactant/Polymer Technology for Daqing EOR. *Spe Reservoir Engineering*, *10*(03), 194–197. https://doi.org/10.2118/27631-pa

GBADAMOSI, A. O., JUNIN, R., MANAN, M. A., & YUSUFF, A. S. (2019) An overview of chemical enhanced oil recovery: recent advances and prospects. *International Nano Letters*, *9*(3), 171–202. https://doi.org/10.1007/s40089-019-0272-8

GOGOI, S. B. (2011) Adsorption–Desorption of Surfactant for Enhanced Oil Recovery. *Transport in Porous Media*, *90*(2), 589–604. https://doi.org/10.1007/s11242-011-9805-y

GUO, Y., LIU, J., ZHANG, X., FENG, R., LI, H., ZHANG, J., XING, L., & LUO, P. (2012) Solution Property Investigation of Combination Flooding Systems Consisting of Gemini–Non-ionic Mixed Surfactant and Hydrophobically Associating Polyacrylamide for Enhanced Oil Recovery. *Energy & Fuels*, *26*(4), 2116–2123. https://doi.org/10.1021/ef202005p

GUPTA, I., RAI, C., & SONDERGELD, C. H. (2020) Impact of Surfactants on Hydrocarbon Mobility in Shales. *SPE Reservoir Evaluation & Engineering*, *23*(03), 1105–1117. https://doi.org/10.2118/201110-pa

LIU, Q., DONG, M. Y., ZHOU, W., AYUB, M., ZHANG, Y., & HUANG, S. (2004). Improved oil recovery by adsorption–desorption in chemical flooding. *Journal of Petroleum Science and Engineering*, *43*(1–2), 75–86. https://doi.org/10.1016/j.petrol.2003.12.017

MAHBOOB, A., KALAM, S., KAMAL, M., HUSSAIN, S., & SØLLING, T. I. (2022). EOR Perspective of microemulsions: A review. *Journal of Petroleum Science and Engineering*, *208*, 109312. https://doi.org/10.1016/j.petrol.2021.109312

Mahdavi, E., & Zebarjad, F. S. (2018) Screening Criteria of Enhanced Oil Recovery Methods. In *Elsevier eBooks* (pp. 41–59). https://doi.org/10.1016/b978-0-12-813027-8.00002-3

Mohyaldinn, M. E., Hassan, A. M., & Ayoub, M. A. (2019) Application of Emulsions and Microemulsions in Enhanced Oil Recovery and Well Stimulation. In *IntechOpen eBooks*. https://doi.org/10.5772/intechopen.84538

Puskas, S. V., L., et al. (2018) *Surfactant-Polymer EOR from Laboratory to the Pilot*. https://doi.org/10.2118/190369-ms

PUSKAS, S. V., et al. (2017) First Surfactant-Polymer EOR Injectivity Test in the Algyő Field, Hungary. In *Proceedings*. https://doi.org/10.3997/2214-4609.201700244

SALAGER, J., FORGIARINI, A., & BULLÓN, J. (2013. How to Attain Ultralow Interfacial Tension and Three-Phase Behavior with Surfactant Formulation for Enhanced Oil Recovery: A Review. Part 1. Optimum Formulation for Simple Surfactant–Oil–Water Ternary Systems. *Journal of Surfactants and Detergents*, *16*(4), 449–472. https://doi.org/10.1007/s11743-013-1470-4

SHENG, J. J. (2015) Investigation of alkaline–crude oil reaction. *Petroleum*, *1*(1), 31–39. https://doi.org/10.1016/j.petlm.2015.04.004

THOMAS, A. (2019. *Essentials of Polymer Flooding Technique*. John Wiley & Sons.

VILLERMAUX, E. (2012) Mixing by porous media. *Comptes Rendus Mecanique*, *340*(11–12), 933–943. https://doi.org/10.1016/j.crme.2012.10.042

WANG, J., YUAN, S., SHEN, P., ZHONG, T., & JIA, X. (2007) *Understanding of the Fluid Flow Mechanism in Porous Media of EOR by ASP Flooding from Physical Modeling*. https://doi.org/10.2523/iptc-11257-ms

ZHONG, H., YANG, T., YIN, H., LU, J., ZHANG, K., & FU, C. (2020) Role of Alkali Type in Chemical Loss and ASP-Flooding Enhanced Oil Recovery in Sandstone Formations. *SPE Reservoir Evaluation & Engineering*, *23*(02), 431–445. https://doi.org/10.2118/191545-pa

UNDERGROUND MINING ENGINEERING 43 (2023) 17-25 UDK 62
UNIVERSITY OF BELGRADE - FACULTY OF MINING AND GEOLOGY ISSN 03542904

Original scientific paper

GEOLOGICAL CHARACTERISTICS OF THE LIMESTONE DEPOSIT "DOBRILOVIĆI"-LOZNICA AND ITS PREPARATION FOR USE IN AGRICULTURE

Vladan Kašić[1], Slavica Mihajlović[1], Nataša Djordjević[1]

Received: March 29, 2023 **Accepted:** June 5, 2023

Abstract:

The paper presents the geological characteristics of the limestone of the "Dobrilovići" deposit and the characterization of the trench sample. The technological scheme of limestone preparation, which is used to obtain suitable sizes for use in agriculture, is presented in the paper. Chemical analysis showed the presence of CaCO3 above 80% and CaO above 44.80%. The content of trace metals is low: Cr 21 mg/kg, Pb 3 mg/kg, and Ni 7 mg/kg. The mean value of the loss of ignition is 39.40%, and the pH is 8.47. Based on the obtained results, it was concluded that the chemical and mineral composition of limestone meets the requirements necessary for the calcification of acidic soils. The results of the determination of the granulometric composition showed the dominant presence of large classes above 50 mm (68%). To obtain a class of 100% -2 mm that meets the requirements for application in the calcification of acidic soils, a technological scheme for the preparation of trench limestone is given, which includes crushing, grinding, and grading.

Keywords: limestone, geological characteristics, agriculture, soil calcification

1 INTRODUCTION

Soil acidity is an important factor that affects the growth of plant crops and can significantly reduce their yield. Most cultivated plants require slightly acidic, neutral to slightly alkaline soils (Jelić et al, 2015). Due to the reduced solubility of biogenic elements (phosphorus and molybdenum) on acidic soils, the yield of plant crops is low. On such land, the content of toxic elements in compounds, especially aluminum, is also increased (Sumner, 2006). The acidity of the soil and the high content of aluminum and heavy metals can be reduced by applying ameliorants based on limestone, this procedure is called calcification. Compounds of calcium and magnesium can neutralize the acidity

[1] Institut za tehnologiju nuklearnih i drugih mineralnih sirovina, Franše ‘dEperea 86, Beograd, Srbija
E-mails: v.kasic@itnms.ac.rs; s.mihajlovic@itnms.ac.rs;
n.djordjevic@itnms.ac.rs

of the soil, which is why limestone-based material is classified as an effective ameliorant (Adams, 1984). Numerous researches in our country and the world indicate that the adequate application of these materials, in combination with organic and mineral fertilizers, is the most effective way of eliminating the unfavorable production characteristics of acidic soils. That is why it is necessary to define amelioration measures when growing most agricultural crops on acidic soils, which will be adapted to both soil properties and climate conditions (Jelić et al, 2015; Jovanović, 2013; Jovanović, 2015).

To apply limestone for the neutralization of acidic soils, the Institute of Agriculture from Loznica carried out geological research and characterization of the limestone of the "Dobrilovići" deposit (Kašić, 2011). Research was started in 2000 by Geozavod - Nemetali from Belgrade and continued in 2001-2004 by the Institute for Technology of Nuclear and Other Minerals from Belgrade. The "Dobrilovići" limestone deposit is located about 150 km southwest of Belgrade, and about 20 km southeast of Loznica, in the atar of the village of Tršić, where it administratively belongs to the Mačva district. The deposit area belongs to the transitional zone of the mountains of the Dinaric system towards the southern peripheral parts of the Pannonian basin.

The "Dobrilovići" limestone deposit is part of the carbonate sedimentary series, formed as part of the sedimentary process on the southern periphery of the former Pannonian Sea. According to the genetic classification of the deposit, it belongs to the exogenous series, the sedimentary group, and the biogenic deposit class. The geological structure of the wider area of the "Dobrilovići" deposit is made up of Palaeozoic, Mesozoic, and Cenozoic formations. Palaeozoic formations are represented by Devonian limestones, sandstones, and shales, followed by Carboniferous limestones, shales, and argillophillites, and Permian carbonate and terrigenous formations. Mesozoic formations are represented by Triassic limestones, sandstones, and clays, subordinated to dolomites, then Jurassic serpentinites, gabbro, and limestones, and Cretaceous massive limestones, sandstones, and quartz-conglomerate-sandstone formation. Cenozoic formations are represented by Neogene and Quaternary formations. Neogene formations consist of Miocene sediments, of which Helvetic sandstones, tuffs, marls and limestones, Tortonian sandy-clay facies and Lajtovac-lithotamnian limestone facies, as well as Pliocene sands, clays, and gravels. Quaternary formations are represented by gravel, sand, and alluvial deposits.

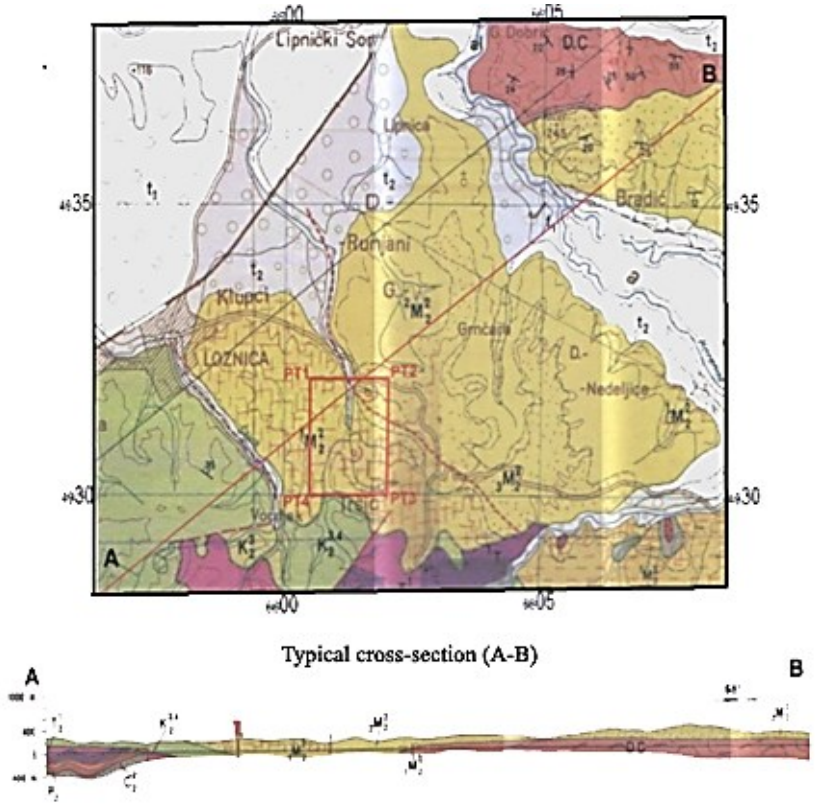

Figure 1 Geological map of the Jadar basin with the investigation area (red box) of the Dobrilovići deposit, Legend: al: alluvium; ${}_3M^2{}_2$: clays, sands, and gravels; ${}_2M^2{}_2$: marly sandstones and marly limestones; ${}^2M^2{}_2$: sandy loams and marls; ${}^1M^2{}_2$: lithotamnian limestones; ${}_1M^2{}_2$: sandy and carbonaceous clays and marls; $K^{3,4}{}_2$: limestones with rudists; $C^2{}_2$: dark gray limestones; D.C.: sandstones; Pz: sandstones, quartzites, phyllites

1.1 Geological structure of the limestone deposit "Dobrilovići"

The "Dobrilovići" limestone deposit was explored in an area of 30 ha. It consists of Middle Miocene sediments, which in the productive part belong to the Lajtovac limestone formation (Mojsilovic, 1968.). In the Middle Miocene deposits of the Jadar basin, to which this area belongs, four facies were observed: (1) gravel, rubble, and larger blocks; (2) layered sandy clays and (3) fine-grained and coarse-grained sands and plastic gray clays with interlayers of coal, remains of plants and molluscs and (4) lithotamnian limestone - Lajtovac. More detailed stratigraphic and paleontological investigations have shown that it is a sparitic limestone with remains of fossil microfauna: Lucina incrassata, Glycimeris pilolus and Solenocurtus sp.

Three layers can be observed in the deposit. The first, youngest layer is represented by clayey carbonate sediments, which contain up to 80% of shells and snails in a gray pelitic

base and thinner interlayers of compact gray limestones. Its greatest thickness is in the central part of the deposit, where it is about 10 m, while it curves around the perimeter. The second layer consists of gray, dark gray to black limestones, which are hard and compact in one part and soft and crumbly in the other. In the central part of the deposits, they have an average thickness of 10 m, with the thickness increasing towards the north and decreasing towards the south. The third deepest and oldest layer consists of typical Lajtovac limestones, which are yellow-white, usually hollow, porous, and soft and with occurrences of decimeter-size compact layers. The greatest thickness of this layer is about 26 m.

1.2 Morphological characteristics of the deposit

The Dobrilovići limestone deposit has a plate-like, layered shape. In the narrowly explored area, the layers are sub horizontal with a northward dip of 3 to 5°. The carbonate stone mass is characterized by significant fissures.

The average thickness of the deposits in the investigated part is about 28 m and in the deepest hole about 45 m. According to OGK data, the thickness of the carbonate series in the wider area of the deposit ranges from 50 to 150 m. The average concentration of reserves in the deposit is about 14.8 m^3 of limestone per m^2 of surface.

The Dobrilovići deposit as a part of the carbonate sedimentary series, was formed as part of the sedimentary process on the southern periphery of the former Pannonian Sea. According to the valid and generally accepted genetic classification of the deposit, it belongs to the exogenous series, the sedimentary group, and the biogenic deposit class.

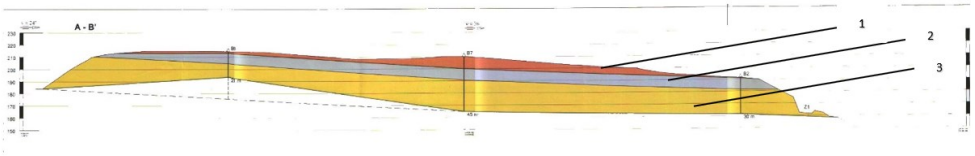

Figure 2 Longitudinal vertical geological cross-section, Legend: 1 - carbonaceous yellow-gray and humic clays; 2 - limestones light to dark gray, of different hardness; 3 - Limestones yellow-white compact, more often hollow and porous

1.3 Tectonic characteristics

Tectonics is not pronounced in the geological area of the Dobrilovići deposit. The primary sub horizontal position of the carbonate layers has been preserved. Only cracks appear and structural elements are layered. There are no traces of fault tectonics in the deposit area.

2 CHARACTERISTICS OF THE MINERAL RAW MATERIAL

The studied characteristics of limestone that are important for application and final valorization include chemical composition, mineral composition, and granulometric composition of the raw material.

Chemical analysis of the Dobrilovići limestone composition showed that the $CaCO_3$ content is higher than 80%, and the CaO content is higher than 44.80%, and the other values are shown in Table 1.

Table 1 The most important components in the limestone of the Dobrilovići deposit (Kašić, 2004)

Component	*content (%) interval (average value)*
CaO	44.20-53.58 (49,51)
MgO	0.25-0.48 (0,39)
SiO_2	2.52-15.78 (8,74)
Al_2O_3	0.49-2.87 (1,10)
Fe_2O_3	0.23-1.24 (0,57)
Na_2O	0.02-0.14 (0,07)
K_2O	0.051-0.51 (0,14)
Loss on ignition	37.80-42.40 (39,40)
$CaCO_3$	80.52-98.05 (90,60)

It was observed that a few metals have a low content: Cr - 21 mg/kg, Pb - 3 mg/kg, and Ni - 7 mg/kg. The presence of Cd was not determined, and the sensitivity of the measurement was less than 0.01 mg/kg. Considering such low contents, these metals do not adversely affect the quality and application of this limestone. The pH value of the limestone showed an interval from 8.2 to 8.7.

The mineral composition of the limestone of the Dobrilovići deposit includes calcite, then quartz, clay minerals, limonite, and others. The most abundant mineral is calcite, which is of organic origin. The granulometric composition of the raw material shows the highest percentage of coarse classes above 50 mm, and the content of the class between 50 and 30 mm is smaller (table 2).

Table 2 Granulometric composition of the raw limestone from the deposit Dobrilovići (Kašić, 2004)

Class of grain size (mm)	*M (%)*	*∑M ↑ (%)*	*∑M ↓ (%)*
- 200 + 100	34	100	34
-100 + 50	34	68	68
-50 + 30	12	32	80
- 30 + 0	20	20	100

Based on the obtained results of the characterization of the limestone of the "Dobrilovići" deposit, it can be concluded that it's chemical and mineral composition meets the requirements necessary for application in agriculture (Sekulić, 2011). The required grain size for these purposes (below 2 mm) requires an adequate technological scheme for its preparation to obtain the appropriate granulometric composition.

3 TECHNOLOGICAL SCHEME OF LIMESTONE PREPARATION OF THE "DOBRILOVIĆI" DEPOSIT

Limestone from the Dobrilovići deposit is intended for correcting the quality of acidic soils, i.e. for increasing its pH value. The best effects are achieved by gradually neutralizing the soil by adding 25 to 50% of the amount needed for complete neutralization of the soil. It is used for basic, deep meliorative, and regular tillage of the soil by spreading evenly over the surface of the dry soil in windless weather. To achieve the full effects of the high productivity of treated soil, it is recommended to use it in combination with organic fertilizers, as well as good homogenization with the surface layer. The size of the particles must be <2 mm. A commercial product of this type made of limestone from the Dobrilovići deposit is called Kalkomel - L.

The technological scheme according to which limestone is prepared (Figure 1) includes crushing, sieving, and grinding until the final fraction below 2 mm is obtained. The raw material GGK 200 mm is brought by truck (1) and unloaded at the depot (2). Using the loader (3), the raw material is transferred to the receiving bunker (4). After that, it is transported using a pendulum feeder (5) to an impact crusher (6) and crushed to a size class of 100% -30 mm. The crushed raw material is transported by a conveyor belt (7) to the vibrating table (8) for sieving and material size class -30 + 2 mm is transported to grinding in the vibrating mill (10) using the conveyor belt (9). The ground product (size class 70% -2 + 0 mm) is returned to the vibrating sieve (8) using the screw conveyor (11). Sieving of the vibrating sieve (8), (size class -2 + 0 mm), falls either on the conveyor belt (12) by which it is transported to the receiving bunker of the packaging device (13), or on the conveyor belt (17) by which it is taken to the finished product

depot (18). The packaged product from the packaging device (13) is placed on pallets (14) and loaded into trucks using a forklift (15). A compressor (16) is provided to operate the packaging device (13). A dedusting filter (19) and a centrifugal fan (20) are provided for dedusting the plant. The hanging transmission (100) is intended for serving the plant.

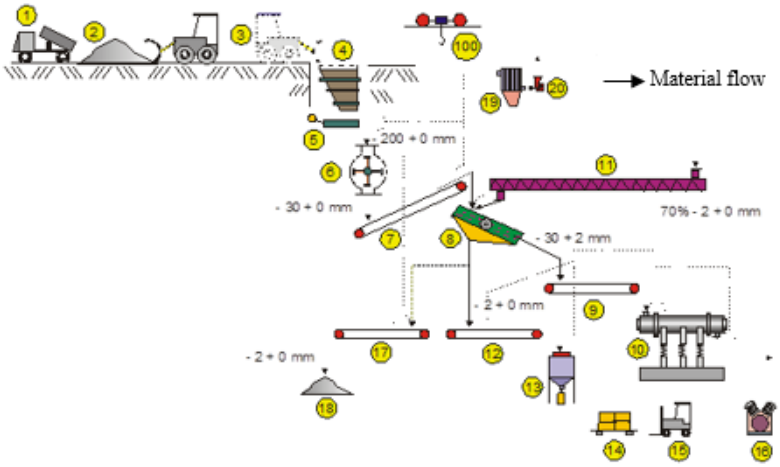

Figure 3 Technological scheme of limestone processing from the "Dobrilovići" deposit, Legend: 1. truck; 2. depot; 3. loader; 4. bunker; 5. dosing table; 6. crusher; 7. conveyor belt; 8. vibrating table; 9. conveyor belt; 10. vibrating mill; 11. screw conveyor; 12. conveyor belt; 13. packing machine; 14. pallets for the finished product; 15. forklift; 16. compressor; 17. conveyor belt; 18. landfill for the finished product; 19. filter for dedusting; 20. centrifugal fan; 100. hanging transmission

The user of this raw material is agriculture, small agricultural producers, as well as large agricultural combines engaged in food production. About 5.1 million hectares are cultivated in Serbia, of which more than 60% belong to acidic soils, with a pH value ranging from 3.5 to 5, so from the perspective of marketing and applying larger quantities of this raw material for the needs of soil calcification, it is very favorable.

4 CONCLUSION

The "Dobrilovići" limestone deposit was explored in an area of 30 ha. The deposit area belongs to the transitional zone of the mountains of the Dinaric system towards the southern peripheral parts of the Pannonian basin. It was formed as part of the sedimentary process on the southern periphery of the former Pannonian Sea. According to the genetic classification, the deposit belongs to the exogenous series, the sedimentary group, and the biogenic deposit class. The geological structure of the wider deposit area is made up of Palaeozoic, Mesozoic, and Cenozoic formations. It is built by Middle Miocene sediments, which in the productive part belong to the Lajtovac limestone formation.

Three layers were observed in the Geological research: the youngest clayey carbonate sediments, then dark gray to black limestones, and older Lajtovac limestones.

Chemical analysis of the limestone of this deposit revealed the presence of CaCO3 above 80%, with the CaO content above 44.80%. The content of trace metals, Cr 21 mg/kg, Pb 3 mg/kg and Ni 7 mg/kg, is low so that they do not adversely affect the quality and application of this limestone. The most common mineral is calcite. The mean value of annealing loss is 39.40%. The pH values ranged from 8.2 to 8.7 with a mean value of 8.47. The results of the determination of the granulometric composition showed the dominant presence of large classes above 50 mm (68%). Based on the obtained results of the limestone characterization of the "Dobrilovići" deposit, it can be concluded that it's chemical and mineral composition meets the requirements necessary for the calcification of acidic soils after the raw material is crushed.

A technological scheme of preparation for obtaining the appropriate granulometric composition (below 2 mm) was conceived. The procedures shown in the technological scheme are crushing, sieving, and grinding. The practical application of the obtained limestone on agricultural plots has shown that the best effects are achieved by gradually neutralizing the soil by adding smaller amounts (25 to 50%) needed for complete neutralization of the soil.

ACKNOWLEDGEMENT

The authors wish to acknowledge the Ministry of Education, Science and Technological Development of the Republic of Serbia for financial support of the research whose results are presented in the paper (contract. 451-03-47/2023-01/200023).

REFERENCES

JELIĆ, M. et al. (2015) Kalcizacija kiselih zemljišta u Centralnoj Srbiji. *Zbornik radova XX Savetovanje o biotehnologiji", Čačak, Srbija, 13.-14. Mart 2015.* Čačak: Univerzitet u Kragujevcu, Agronomski fakultet Čačak, pp. 51-58.

SUMNER, M.E. (2006) Food production on acid soils in the developing world: problems and solutions. *Soil Science and Plant Nutrition*, 51 (5), pp. 621-624. DOI:10.1111/j.1747-0765.2005.tb00077.x

ADAMS, F. (1984) *Soil acidity and liming*. Madison, WI, American Society of Agronomy.

JOVANOVIĆ, V., et al. (2013) Mechanical properties of limestone briquettes with bentonite for calcification of acid soil. In: *Proceedings of 5th Balkan mining congress,*

Ohrid, Macedonia, 18.-21. September 2013. Ohrid: Association of Mining and Geological Engineers of Macedonia, pp. 404-408.

JOVANOVIĆ, V. et al. (2015) Mechanical properties of limestone briquettes and pellets with bentonite for calcification of acid soil. In: *Proceedings of XVI Balkan Mineral Processing Congress, Belgrade, Serbia, 17-19 June 2015*. Belgrade: Mining Institute Belgrade, Academy of Engineering Science of Serbia-Department for Mining, Geology and Systems Sciences and University of Belgrade, pp. 1083-1086.

KASIĆ, V**.** et al. (2011) Geology of the deposit of limestone Dobrilovici near Loznica (Serbia). In: *Proceedings of the 43rd International October Conference on Mining and Metallurgy, Kladovo 12-15. 10. 2011*. Bor: Technical Faculty, University of Belgrade and Mining and Metallurgy Institute Bor, Serbia, pp. 383-389.

KAŠIĆ, V. (2004) *Elaborat o rezervama krečnjaka u ležištu Dobrilovići KO Tršić, Loznica*. 94 s, Beograd: Institut za tehnologiju nuklearnih i drugih mineralnih sirovina.

SEKULIĆ, Ž. (2011) *Kalcijum karbonatne i kvarcne mineralne sirovine i njihova primena*, Beograd: Institut za tehnologiju nuklearnih i drugih mineralnih sirovina.

JOVANOVIĆ, V. (2016) *Izučavanje procesa okrupnjavanja mlevenog krečnjaka radi primene u poljoprivredi*, Doktorska disertacija, Rudarsko-geološki fakultet Univerziteta u Beogradu.

MOJSILOVIĆ S. et al. (1968) Tumač za OGK, list Zvornik 54, Savezni geološki zavod, 47 s, Beograd

UNDERGROUND MINING ENGINEERING 43 (2023) 27-41 UDK 62
UNIVERSITY OF BELGRADE - FACULTY OF MINING AND GEOLOGY ISSN 03542904

Review paper

CRITERIA FOR EVALUATION THE SEISMIC EFFECT OF BLASTING

Suzana Lutovac[1], Miloš Gligorić[1], Jelena Majstorović[1], Milanka Negovanović[1], Saša Jovanović[2]

Received: October 30, 2023 **Accepted:** December 06, 2023

Abstract:

The explosion that caused by blasting is accompanied by the release of a large amount of energy. That energy can be used for rock mass destruction. At the same time, one part of that energy is utilized for rock destruction while the second one gets lost in the rock mass in the form of seismic wave. Regarding that, blasting effects can be divided into two categories such as: useful work and useless work. Useful work is manifested in form of crushing and milling of the rock material in the limited zone around explosive matter and is defined as brisant effect of explosion. Useless work is a phenomenon known as seismic effect of explosion. Useless work is associated with the elastic displacement i.e., the oscillation of the rock mass particles in a very large space around the place of explosion and is felt as a shock. Oscillation velocity of the induced rock mass is most often taken as the parameter for the evaluation the seismic effect of blasting. It is considering that the oscillation velocity best relates and describes the danger of shocks and damages which can be caused, so the appropriate standards for the shock protection are based on the data related to the oscillation velocity. In many countries, regulations that control the shock level caused by blasting activities have been adopted. For our country, these regulations have not yet been adopted, so we used the regulations of other countries to solve these problems. In this paper, criterion of the Institute of Physics of the Earth, Russian Academy of Sciences, criterion according to the Russian standards for mining objects, criterion according to the German standards DIN and criterion according to the USA standards are presented.

Keywords: blasting, seismic effect, oscillation velocity, criterion for the damage evaluation

1 INTRODUCTION

Explosion, that caused by detonation of explosive materials, is accompanied by the release of a large amount of energy. That energy manifests a huge strength in short time intervals and can be used for rock mass destruction. One part of that energy is used for

[1] University of Belgrade, Faculty of Mining and Geology
[2] University of Priština in Kosovska Mitrovica, Faculty of Technical Sciences
Emails: suzana.lutovac@rgf.bg.ac.rs, milos.gligoric@rgf.bg.ac.rs, jelena.majstorovic@rgf.bg.ac.rs, milanka.negovanovic@rgf.bg.ac.rs, sasa.m.jovanovic@pr.ac.rs

rock destruction and the other part gets lost in the rock mass in the form of seismic wave. Seismic waves caused by blasting act in the same way and have the same character as seismic waves caused by an earthquake. What makes seismic waves caused by an earthquake and by explosive different from each other is: the energy they transmit, range of influence, time of duration, frequency dynamic characteristic of seismic waves (Peng et al., 2019).

What additionally differentiates an uncontrolled explosion in the Earth's crust – related to earthquakes, from a controlled explosion – related to detonation of explosive materials, is the knowledge of the energy that is released on that occasion. In the case of an earthquake, we get to the amount of the energy that is released only after it has happened and after determining the consequences of its effect. In the case of detonation of explosive material, we know in advance the amount of energy that is released, and we can define the part that will be the carrier of seismic shock. Thanks to this possibility, it is possible to estimate the range and intensity of the seismic wave for controlled explosions (Dao et al., 2021).

2 EXPLOSION EFFECT ON WORKING ENVIRONMENT

During the explosion, one part of the energy is used for rock mass destruction and the other part of the energy gets lost in the rock mass in the form of seismic wave. Depending on distance from the center of explosion, different changes occur in the rock mass. In a homogeneous and isotropic environment, three zones can be distinguished:

-crushing zone,
-destruction zone and
-shock zone.

In the crushing zone, the shock wave exerts pressure on the surrounding rocks at a velocity greater than the sound velocity, while in the zone around the explosion space, at a distance (3–7)r, where r is the radius of explosive charge, the rock material gets crushed and compressed into the rock mass. The resulting pressure multiple overcomes the compressive strength of the rock, from 40 to 400 times. In this zone, rock crushing is the most intensive and the largest amount of the available energy is consumed.

Destruction zone occurs at a distance greater than (3–7)r. In this zone, the shock wave is significantly weakened and moves at the sound velocity. It causes stresses in the surrounding rock materials which resulting in the creation of cracks of different directions and orientations. Radial and concentric cracks or their combinations are formed.

Shock zone occurs when the shock wave is weakened so much that it is able to only move particles in the domain of elastic deformations. In this zone, there is no destruction

but a rock mass particles displacement which is felt as shock. Elastic waves that propagate in this zone have the nature of seismic waves.

From the point of view of exploitation, when the rock is destructed by explosive, the crushing zone and destruction zone are important. The third zone, in which only particles move in the domain of elastic deformations, is also known as seismic zone. This zone does not affect the destructions effects but can be harmful to objects in the environment, both on the surface and underground.

A representation of the deformation zones during the explosion is given in Figure 1. Deformation zones because of explosion in homogeneous and solid rock mass are shown in Figure 1a. In such environments, three deformation zones are clearly observed: crushing zone, destruction zone and shock zone. During the blasting activities in soft, plastic, and unbound rock material, the following zones should be distinguished: extrusion zone, plastic deformation zone and elastic deformation zone, which are shown in Figure 1b. In such environments, the extent of destruction under the influence of stresses caused by shock wave is insignificant due to their plastic properties.

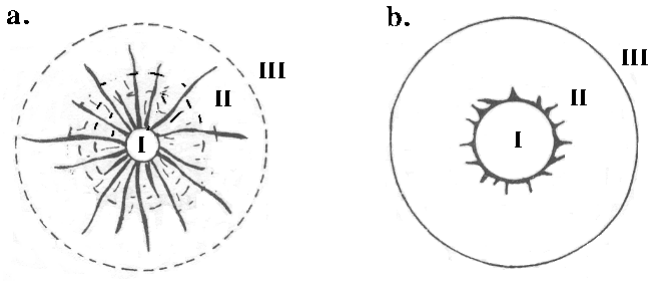

Figure 1 A representation of deformation zones during explosion:
a. in homogeneous and solid rock material, I – crushing zone, II – destruction zone, III – shock zone
b. in plastic and unbound rock material, I – extrusion zone, plastic deformation zone, III – elastic deformation zone

Blasting effects can be divided into two categories:

-useful work and

-useless work.

Useful work is manifested in the form of crushing and milling of the rock material in the limited zone around explosive matter and is defined as brisant effect of explosion. Work related to the crushed rock material displacement by products of explosion i.e., by gases is defined as fugitive effect of explosion.

Useless work is a phenomenon known as seismic effect of explosion. Work is related to elastic displacement i.e., the oscillation of the rock mass particles in a very large space around the place of explosion.

3 PARAMETERS OF THE ROCK MASS OSCILLATION

When a seismic wave hits a point in the terrain, it pushes the soil particles at that point out of their equilibrium position and they oscillate around their equilibrium position for a certain time until they completely settle down. Particles oscillation of the rock material (terrain or soil) is what manifests itself and is felt as a shock, i.e., soil vibration.

The waves move at high velocities through the rock mass (300 –7000 m/s), at long distances, inducing the particles oscillation at the points they encounter. The material particles of the mass do not move anywhere, but only oscillate around their equilibrium position at much lower velocities, of the order of mm/s, until the oscillations are dampened, i.e., until the rock mass settles.

Shock intensity caused by blasting activities can be established by measuring one of the three basic parameters that characterize oscillation of induced soil, those are:

- rock mass particles displacement x is the distance where the particle moves away from its equilibrium position during the oscillation. It is expressed in mm or in parts of mm.
- oscillation velocity of the rock mass particles v is the displacement velocity of the particles during the oscillation. It is expressed in mm/s or cm/s.
- acceleration of the induced environment a show the degree of change of the oscillation velocity i.e., particles displacement

The magnitudes of these three parameters indicate the force intensity with which they were caused, and therefore the degree of danger caused by the shock. These parameters represent the basic dynamic parameters of the shock. Oscillation velocity of the induced rock mass is most often taken as the parameter for the evaluation of the seismic effect of blasting. It is considered that the oscillation velocity best relates and describes the danger of shocks and damages which can be caused, so the appropriate standards for the shock protection are based on the data related to the oscillation velocity.

4 ROCK MASS OSCILLATION VELOCITY EQUATION

Rock mass oscillation velocity equation defines velocity alteration of rock mass oscillation depending on distance, explosive amount, properties of rock material and blasting method. The equation, defined in this way, offers the possibility to determine the seismic effect of blasting towards a structure, whereby the connection between the rock mass oscillation velocity and consequences that can affect facilities, is used.

The equation of M.A Sadovskii (Medvedev, 1964) is given in the form

$$v = K \cdot R^{-n} = K \cdot \left(\frac{r}{\sqrt[3]{Q}}\right)^{-n} \quad (1)$$

where there are:

v – rock mass oscillation velocity $[cm/s]$,

K – coefficient conditioned by rock mass characteristics and blasting conditions,

n – exponent conditioned by characteristics of rock mass and blasting conditions,

r – distance from the blasting site to the monitoring point $[m]$,

Q – total amount of explosive $[kg]$,

R – the reduced distance, given in the form $R = \frac{r}{\sqrt[3]{Q}}$.

The Sadovskii equation is determined based on test blasting for the concrete working environment.

In the Equation (1) two parameters appear, K and n, which need to be determined for a specific work environment and specific blasting conditions. The Least Square Method is mainly used to obtain the parameters K and n which represents a common model (Simeunović, 1985).

5 DAMAGE EVALUATION OF THE BLASTING

Explosive materials in mining, geology, construction, and other industries, with their effect, disrupt the natural environment in the form of crushing, scattering pieces of rock, air strikes, occurrence of seismic effects, etc.

The basic requirement for the use of explosive devices is that the mentioned effects do not adversely affect people who have direct or indirect contact with the environment within the minefield, as well as that they do not damage residential or industrial buildings that can be found in the field of their effect.

In most countries, regulations have been adopted that regulate the level of shock caused by blasting, which can load buildings, depending on their importance, condition, and dynamic resistance. The regulations are in accordance with the seismic and geological conditions, which are characteristic of a particular country. Such regulations have not yet been adopted for our country, so in solving this problem we use the regulations and norms of other countries, most often Russian, German, and American.

Before blasting activity, it is necessary to perform the categorization of the condition of the objects located in the immediate vicinity of the blasting site, according to their resistance to shocks and oscillations. According to this criterion, all objects are classified into three basic categories, and they refer to buildings that were not built according to regulations.

Type A. This type includes buildings that were built from raw stone, rural buildings from unbaked bricks, buildings with walls plastered with mud, which practically means that they are the least resistant to shocks and vibrations.

Type B. This type includes buildings made of baked bricks, buildings built of blocks and prefabricated buildings (from prefabricated materials), buildings made of natural hewn stone, as well as buildings with partially wooden construction.

Type C. This type of construction includes buildings built with reinforced concrete construction and well-built wooden houses. This type of building is also the most resistant to shocks and vibrations.

In order to define the condition of the object, it is necessary to determine the degree of object damage. Damages on objects are classified into five degrees.

I degree – light damages. Small cracks in the plaster. Lime falling off the ceilings, small pieces of plaster falling off.

II degree – moderate damages. Small pieces of plaster falling from the ceiling and walls, small cracks in the walls, tiles falling from the roof, parts of the chimney falling from the roof.

III degree – hard damages. Deep cracks in the walls, delamination and falling of the ceiling, chimney falling from the roof.

IV degree – destruction. Open cracks in the walls, demolition of parts of the building, breaking of connections between individual parts of buildings, demolition of internal walls of buildings.

V degree – absolutely destruction. Complete separation of the structure and demolition of the building.

5.1 Criteria for shock evaluation of the blasting

Shock intensity caused by blasting is sometimes evaluated using a scale applied in seismology, most often the Mercalli – Cancani – Sieberg (MCS) scale. Although there is a similarity between shocks caused by blasting and earthquakes, the differences are significant especially during the duration of the earthquake and period of oscillation (Anas et al., 2022). Those differences exclude the possibility of applying the MCS scale for shock intensity evaluation caused by blasting. Today in the world there are many specialized scales for shock intensity evaluation caused by blasting (Savić, 2000).

5.1.1 Criterion of the Institute of Physics of the Earth, Russian Academy of Sciences[3]

The permissible shock intensity for objects of different resistivity is related to rock mass oscillation velocity. The degree of seismic intensity is given in the form of twelve seismic degrees. Russian scale for shock evaluation caused by blasting is established in the Institute of Physics of the Earth, Russian Academy of Sciences. The evaluation of the seismic intensity of shock is given in Table 1.

Table 1 The evaluation of the seismic intensity of shock according to criterion IFZ Russia

Oscillation Velocity $v[cm/s]$	Level of seismic intensity I	Description of actions
To 0,2	I	Action is revealed only by instruments
0,2–0,4	II	Action is felt only in some cases when there is a complete silence
0,4–0,8	III	Action is felt by very few people or only those who are expecting it
0,8–1,5	IV	Action is felt by many people, the clink of the windowpane is heard
1,5–3,0	V	Plaster fall, damage on buildings in poor condition
3,0–6,0	VI	Air cracks in plaster, damage, damage to buildings that already have developed deformations
6,0–12,0	VII	Damage on the buildings in good condition, cracks in plaster, parts of the plaster fall down, air cracks in walls, cracks in tile stoves, chimney wrecking
12,0–24,0	VIII	Considerable deformations on buildings, cracks in bearing structure and walls, bigger cracks in partition walls, wrecking of factory chimneys, fall of the ceiling
24,0–48,0	IX	Wrecking of buildings, bigger cracks in walls, exfoliation of walls, collapse of some parts of the walls
greater than 48,0	X – XII	Bigger destruction, collapse of complete structures etc.

[3] Федеральное государственное бюджетное учреждение науки Институт физики Земли им. О.Ю. Шмидта Российской академии наук (ИФЗ РАН)

As it can be seen from Table 1, damage on the buildings appears when oscillation velocity caused by blasting exceeds the IV level of the seismic scale. Damage on the buildings in poor condition can occurs during the shock with the intensity of the V level of seismic scale, while for buildings in good condition, the considerable deformations can only be expected during the VII level of the seismic scale. According to that, for the evaluation the seismic effect of blasting for buildings and other objects, it is necessary to take into account the condition of objects, the characteristics of soil as well as the number and method of blasting.

The permissible oscillation velocity for construction objects (residential, industrial, etc.) also depends on the type of object, its importance and purpose. Regarding that, all construction objects are divided into four classes.

I class. Especially significant objects of republican importance and architectural monuments. Blasting next to such objects is possible only in exceptional cases.

II class. Industrial facilities of exceptional importance: pipelines, large factory halls, hoist towers, water towers, and similar facilities; facilities whose useful life is longer than twenty to thirty years; residential buildings where a large number of inhabitants live, centers of culture, cinemas and similar facilities.

III class. Industrial facilities and administrative buildings of relatively small dimensions, the height of which does not exceed three floors; mechanical workshops, compressor stations and similar facilities; residential buildings where a small number of people live; warehouses, etc.

IV class. Buildings and industrial facilities where expensive machines and devices are located, and their damage does not endanger the life and health of people; warehouses, automobile bases, cold storage buildings, compressor stations, etc.

The permissible oscillation velocities in the foundation of objects, depending on object class, are given in Table 2.

Table 2 The permissible oscillation velocities in the foundation of objects depending on object class

Characteristics of the buildings and objects	The permissible oscillation velocity per object class, $v[cm/s]$		
	II	III	IV
Residential buildings and industrial buildings with reinforced concrete or steel construction, with light filling, calculated on seismic impacts. Satisfactory construction quality and without any changes in relation to the project and budget. There are no residual deformations in the construction.	5,0	7,0	10,0
Residential buildings and industrial buildings with reinforced concrete or steel construction. There are no residual deformations in the construction.	2,0	5,0	7,0
Buildings with partition walls made of brick or stone. New or old stone buildings or masonry buildings built without seismic influences. Good construction quality. There are no residual deformations in the construction.	1,5	3,0	5,0
Buildings that have significant wall damage and structural cracks. New or old stone or brick buildings with minor unconnected cracks in load-bearing and partition walls.	1,0	2,0	3,0
Old or new buildings with cracks and broken connections between individual elements. Stone or brick buildings with oblique cracks in load-bearing walls and corners, etc.	0,5	1,0	2,0
Damaged reinforced concrete construction, large cracks in the concrete. Buildings where the load-bearing walls have a large number of cracks, damaged connections between the external and internal walls, etc. Buildings built from prefabricated elements that are not seismically secured.	0,3	0,5	1,0

Criteria according to Russian scale for mining facilities. The level of rock mass deformation plays an important role in the protection of mining facilities constructed in

a rock mass such as shafts, drifts, tunnels, rise headings, dip headings, chambers, stopes, sublevel posts, hydro-engineering tunnels, bench slopes, etc. Deformation characteristics of a rock mass have an essential impact while determining the threshold of deformations for facilities constructed in the rock mass (Lutovac et al., 2016). On the basis of experimental measurements, there have been established oscillation velocities of the rock mass in varied mining-geological and mining-engineering conditions whose values (Russian standards) are presented in Table 3.

Table 3 Description of occurrences in rock mass induced by seismic wave

Description of occurrences in rock mass induced by seismic wave	Oscillation velocity v $[mm/s]$
There are no damages	< 20
The occurrence of insignificant development of fissures induced by previous blasting; locally, falling out of single pieces along previously weakened surfaces.	20 – 50
Intensive development of existing fissures followed by minor caving of rock pieces with the dimensions to 0.2x0.2x0.2 m; the occurrence of cracks in tectonically weaker material filled fissures; the caving of bench slopes along tectonic deformations.	50 – 100
The development of tectonic fissures and the caving of rock pieces with the dimensions 0.5x0.5x0.5 m.	100 – 150
Caving from sides and roof of underground chambers along tectonic fissures, the formation of new fissures in undamaged part of the rock mass, collapse of safety pillars and benches.	150 – 300
Complete damage of sides and roof of chambers followed by large blocks with dimensions of 1x1x1m and filling up to the half of constructed surface; caving of hard rock slopes	300 – 400
Complete demolition of rock mass, the caving of large blocks bigger than 1x1x1 m and covering up more than a half of the chamber.	> 400

5.1.2 Criteria according to German DIN standard

These criteria prescribe the maximum permissible values of soil oscillation velocities, depending on the importance and condition of the objects, for oscillation frequencies of 5-100 Hz and for one to two blasting per day. The maximum permissible soil oscillation velocities are given in Table 4.

Table 4 Maximum permissible values for oscillation velocity v and oscillation frequency according to DIN

Maximum permissible values of oscillation velocity $\boldsymbol{v}[\boldsymbol{mm/s}]$				
Type of the structure	Foundation			Top floor ceilings
	<10 Hz	10–50 Hz	50–100 Hz	All frequencies
1. Structures used for craftsmanship, industrial and similar structural structures.	20,0	20,0–40,0	40,0–50,0	40,0
2. Residential buildings and structures similar in construction or function.	5,0	5,0–15,0	15,0–20,0	15,0
3. Structures that because of their special sensitivity to vibrations do not fall into groups 1 and 2 and are essential for conservation (for institutions as cultural-historical monuments).	3,0	3,0–8,0	8,0–10,0	8,0

Graphical representation of $DIN-4150$ standard, shock as a function of frequency, is shown in Figure 2.

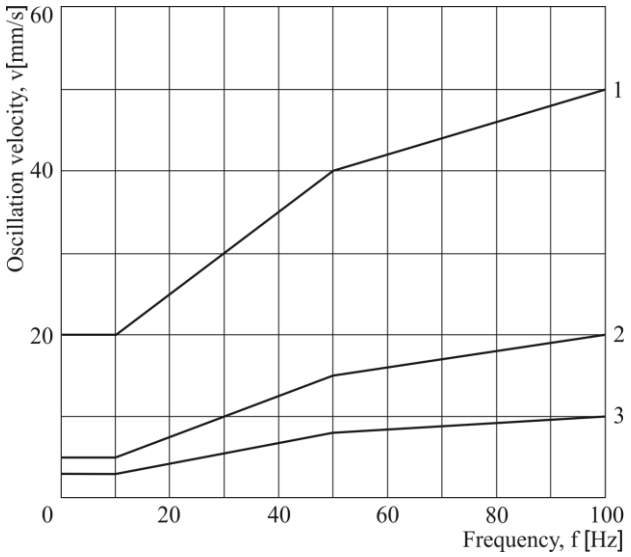

Figure 2 Graphical representation of $DIN-4150$ standard (1, 2 and 3-type of the structure) (DIN 4150-3:1999)

5.1.3 Criterion according to USA standard

The United States Bureau of Mines (USBM) has issued a standard (RI 8507-1980) for permissible oscillation velocities of residential buildings as a function of frequency. For residential buildings, the permissible oscillation velocities in the frequency range of $1-4\,Hz$ vary from $4-20\,mm/s$. In the frequency range of $11-30\,Hz$, the permissible oscillation velocities vary from $20-50\,mm/s$, and above $30\,Hz$ they amount to $50\,mm/s$. Graphical representation of the limit oscillation velocities is demonstrated in Figure 3.

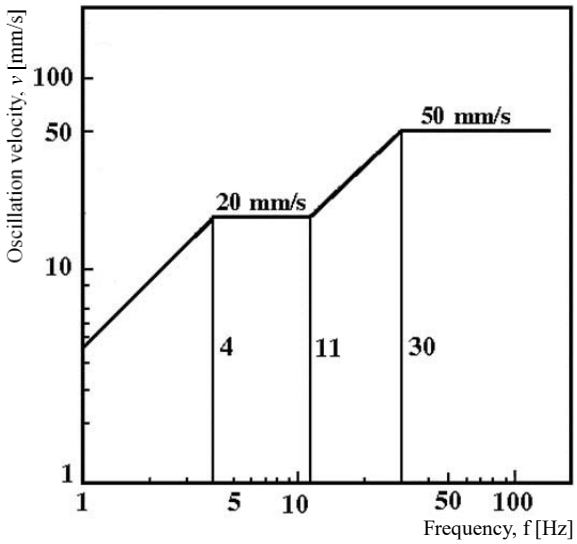

Figure 3 Graphical representation of the limit oscillation velocities - The United States Bureau of Mines RI 8507 (Siskind et al., 1980)

6 CONCLUSION

In the mining industry, explosives are primarily used to extract minerals from hard rocks. In the world today, explosives charges with a very large amounts of explosive are used which are capable to cause seismic shock of such intensity, which will a harmful effect on the environment and induce the displacement of objects.

In most countries, regulations have been adopted that regulate the level of shock caused by blasting, which can load buildings, depending on their importance, condition, and dynamic resistance. Such regulations have not yet been adopted for our country, so in solving this problem we use the regulations and norms of other countries, most often Russian, German and American.

In this paper, criterion of the IFZ Russian Academy of Sciences, criterion according to Russian norms for mining facilities, criterion according to German DIN standard and criterion according to USA standard are represented.

According to criterion of the IFZ Russian Academy of Sciences, the permissible intensity of shock for objects of different resistivity is related to rock mass oscillation velocity. The degree of seismic intensity is given in the form of twelve seismic degrees.

Criteria according to German DIN standard prescribe maximum permissible values of soil oscillation velocity, depending on the importance and condition of objects, for three

groups of objects, for the frequency range of $5 - 100\ Hz$ and for one to two blasting per day.

Criterion according to USA standard prescribes the permissible oscillation velocities of the residential buildings in the appropriate frequency range.

Given that the regulations regulating the level of shock caused by blasting are in accordance with the seismic and geological conditions that are characteristic of a certain country, the necessity of regulating this phenomenon in our regulations is indicated. In this way, doubts would be avoided when evaluating the seismic effect of the explosion, which occurs because of blasting.

REFERENCES

ANAS, S. M., ALAM, M., and UMAIR, M. (2022) Air-blast and ground shockwave parameters, shallow underground blasting, on the ground and buried shallow underground blast-resistant shelters: a review. *International Journal of Protective Structures*, *13*(1), pp. 99-139.

DAO, H., PHAM, T. L., and HUNG, N. P. (2021) Study on an online vibration measurement system for seismic waves caused by blasting for mining in Vietnam. *Journal of Mining and Environment*, *12*(2), pp. 313-325.

DIN 4150-3:1999 (1999) *Structural Vibration. Part 3: Effects of Vibration on Structures*; DIN Deutsches Institut für Normung: Berlin, Germany.

LUTOVAC, S., TOKALIĆ, R., GLUŠČEVIĆ, B., VIDANOVIĆ, N. and BELJIĆ, Č. (2016) Effect of blasting on the adjacent building and mining structures at the open pit Kijevo, In: *Proceedings of the 24th International Conference "ECOLOGICAL TRUTH" Eco-Ist'16*, Vrnjačka Banja: University of Belgrade - Technical Faculty in Bor, pp. 148-155.

MEDVEDEV, S.V. (1964) *Seismic of Mountainous Explosions*. Nedra Publisher: Moscow, Russia, pp. 42–43.

PENG, Y., SU, Y., WU, L., and CHEN, C. (2019) Study on the attenuation characteristics of seismic wave energy induced by underwater drilling and blasting. *Shock and Vibration*, *2019*, 4367698, pp. 1-13.

SAVIĆ, M. (2000) *Blasting at of the Open Pits*. Monograph, RTB Bor, Cooper Institute Bor, Indok Center: Bor, Serbia, pp. 317–319.

SIMEUNOVIĆ, D. (1985) *Mathematics.* Faculty of Mining and Geology, Mining Department: Belgrade, Serbia, pp. 101–103.

SISKIND, D. E., STRACHURA, V. J., STAGG, M. S., and KOPP, J. W. (1980) *Structure response and damage produced by airblast from surface mining*. US Department of the Interior, Bureau of Mines: New York, NY, USA

UNDERGROUND MINING ENGINEERING 43 (2023) 43-70 UDK 62
UNIVERSITY OF BELGRADE - FACULTY OF MINING AND GEOLOGY ISSN 03542904

Original scientific paper

MITIGATING HYDRATE FORMATION IN ONSHORE GAS WELLS: A CASE STUDY ON OPTIMIZATION TECHNIQUES AND PREVENTION

Milica Ješić[1], Bojan Martinović[1], Stefan Stančić[1], Miroslav Crnogorac[2], Dušan Danilović[2]

Received: November 22, 2023 **Accepted:** December 15, 2023

Abstract:

Gas wells, particularly those situated onshore, play a vital role in the global energy sector by supplying a significant portion of natural gas. However, operational challenges, notably gas hydrate formation, pose substantial issues, leading to complications such as flowline blockages and unexpected well shutdowns. Gas hydrates, crystalline structures resembling ice, form under specific conditions of low temperature and high pressure. This paper explores the complex process of hydrate formation in gas wells, emphasizing the challenges it presents and the need for specialized strategies to address these issues.

The primary focus is a case study of an onshore gas well experiencing recurrent hydrate-related problems. Leveraging PipeSim software, a well model is developed, followed by a sensitivity analysis under various operational scenarios. The study investigates mitigation strategies, including choke position adjustments and methanol introduction, crucial for the safe production of oil and gas fields.

The significance of this study lies in its aim to optimize well performance and mitigate risks associated with hydrate formation. Findings contribute to existing knowledge and offer practical solutions for industry practitioners and researchers dealing with onshore gas wells. The paper's structure includes a review of related work, details on the experimental setup and results, and concluding remarks.

The perennial challenge of hydrate formation in gas wells necessitates a case-specific assessment and individualized approaches. Nodal analysis and well modeling software have become indispensable tools for engineers in developing preventative measures. This paper presents a methodological approach using a specific well as an example, evaluating the effectiveness of three methodologies: downhole choke installation, methanol dosing, and well transfer to a high-pressure separator.

Keywords: Gas Well, Gas Hydrate Formation, Well Modeling, Well Performance Optimization, Choke Position Adjustments, Methanol Injection

[1] NTC NIS Naftagas doo, Narodnog fronta 12, 21000 Novi Sad
[2] University of Belgrade - Faculty of Mining and Geology, Djusina 7, Belgrade, Serbia
E-mails: milica.jesic@nis.rs; bojan.martinovic@nis.rs; stefan.stancic@nis.rs; miroslav.crnogorac@rgf.bg.ac.rs; dusan.danilovic@rgf.bg.ac.rs

1 INTRODUCTION

Gas wells, especially those located onshore, are integral components in the global energy sector, providing a substantial source of natural gas. These wells, however, are susceptible to various operational challenges, with gas hydrate formation being a predominant issue ("Gas Hydrate Control," 2015; Makagon 1997). Gas hydrates are crystalline ice-like structures that form under specific conditions of low temperature and high pressure, often leading to complications such as blockages in the flowlines and unexpected well shutdowns.

The formation of hydrates in gas wells is a complex process that occurs under specific conditions of high pressure and low temperature. When natural gas, which contains methane, ethane, propane, and other similar components, flows through a gas well, these gases have the potential to physically combine with water molecules present in the fluid. Under the influence of high pressure, a hydrate crystal lattice is formed, capturing gas molecules within its structure. This process results in the formation of solid hydrates that can accumulate in wells. It is important to note that the presence of certain conditions, such as low temperatures and enough water, is crucial for the formation of hydrates in gas wells. The absence of any of these conditions prevents their occurrence. This phenomenon can pose significant challenges in the exploitation of gas resources, necessitating the development and implementation of specialized strategies to avoid potential operational difficulties caused by the presence of hydrates. (Sloan, 2010; Straume et al., 2016).

The primary objective of this paper is to present a comprehensive case study of an onshore gas well that has been experiencing recurrent issues related to hydrate formation. Through the utilization of PipeSim software, a base model of the well was meticulously developed. This was followed by a sensitivity analysis focusing on hydrate formation under various operational scenarios. The study further explores and analyzes different mitigation strategies, including the adjustment of choke positions and the introduction of methanol. Understanding and predicting gas hydrate formation is crucial for the safe production of oil and gas fields (Duan et al., 2023).

This study is significant as it aims to optimize the well's performance and mitigate the risks associated with hydrate formation. The findings of this study will not only contribute to the existing body of knowledge but will also provide valuable insights and practical solutions for industry practitioners and researchers dealing with onshore gas wells.

The remainder of the paper is structured as follows. Section 2 highlights related work. The experimental setup and its results from real-world applications are detailed in sections 3 and 4, respectively. Finally, conclusions are presented in section 5.

2 RELATED WORK

Musakaev and Borodin (2021) conducted mathematical modeling of gas hydrate formation in a zonal heterogeneous porous reservoir. Their work provides insights into the process of gas hydrate formation in different zones of a reservoir, which is crucial for understanding and predicting hydrate-related issues in onshore gas wells.

A study by Wang et al. focused on hydrate formation during the intervention operations of deepwater high temperature and pressure gas wells. Although their study is based on deepwater wells, the established temperature-pressure coupling model and the physical simulation experiment of hydrate formation provide valuable insights that can be applied to onshore gas wells under specific conditions. Shukla, Singha, and Sain (2022) worked on modeling in-situ horizontal stresses and orientation of maximum horizontal stress in gas hydrate-bearing sediments in the Mahanadi offshore basin in India. While their study is based on offshore basins, the modeling techniques and findings can be insightful for understanding stress orientations in onshore gas hydrate-bearing sediments.

Hashemi et al. (2019) conducted an experimental study and modeling of the kinetics of gas hydrate formation for various hydrocarbons in the presence and absence of SDS. Their work provides valuable data and insights into the kinetics of hydrate formation, which is crucial for developing effective hydrate management strategies in onshore gas wells. The formation of gas hydrates in onshore gas wells is a significant operational challenge, necessitating effective management strategies (Song et al., 2020). Song et al. conducted a study focusing on deepwater gas well testing operations in the South China Sea, providing valuable insights into hydrate management strategies. The study explored three strategies: thermodynamic hydrate inhibitor (THI) injection, hydrate slurry flow technology, and kinetic hydrate inhibitor (KHI) injection. Each strategy presents unique advantages and challenges that are crucial for industrial applications.

Nwankwo (2019) presented a case study of an onshore gas well that was crucial for fueling a flow station. The well experienced frequent shutdowns, not due to equipment failures but because of the Joule-Thompson effect. Through the development of a temperature-sensitive production performance model, the study found that immediate chemical hydrate inhibition was not necessary. Adjusting the choke size to increase flow line pressure allowed the well to operate in a non-hydrate formation region, ensuring stable production.

A recent study by Ping et al. (2022) focused on evaluating the risk of gas hydrate formation in ESP-Lifted Natural Gas Hydrate Wells. The study established a gas-liquid two-phase flow model to predict the hydrate formation region in dedicated gas/water lines and mixing-delivery lines. The research provided insights into the influence of the operating frequency of Electric Submersible Pumps (ESP) and the power of heaters on temperature and pressure in the wellbore, contributing to the understanding and mitigation of the risk of secondary hydrate formation in ESP-lifted wells.

Wei, Jiang, Zhao, Zhou, Zhang, Li, Sun, and Li (2021) present a theoretical model for the non-equilibrium formation and decomposition of hydrates in marine gas/water-producing wells. The model is based on a phase equilibrium model of methane hydrate and a kinetic model of hydrate formation and decomposition. The authors also develop a wellbore temperature and pressure distribution model for water-bearing natural gas recovery. Numerical simulations are used to verify the accuracy of the theoretical model and to study the factors that affect hydrate formation and decomposition.

3 METHODOLOGY

The methodological framework employed in this study comprises four key steps, each meticulously designed to ensure a robust and systematic approach to our research objectives. The following sections outline the sequential stages of our methodology: Data Collection, Creating and Matching the Model, Performing Sensitivity Analysis, and Finalizing Results. Each step is integral to the comprehensive understanding and interpretation of the data, contributing to the reliability and validity of our findings. The schematic representation below (Figure 1) illustrates the interconnected nature of these methodological components, emphasizing the seamless flow from data collection to the conclusive interpretation of results.

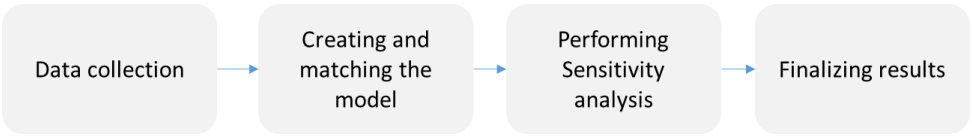

Figure 1 Schematic representation of methodology

3.1 Data Collection

Data for this study were sourced directly from an operational onshore gas well experiencing issues with hydrate formation. The dataset encompasses various parameters crucial for the analysis, including pressures and flow rates (Table 1) and gas composition (Table 2). In Table 3, the results of relevant hydrodynamic measurements are presented, more precisely, measurements of dynamic pressure stages in the wellbore and pressure gradient. The current equipment at the well is described in Table 5, where information about the production downhole equipment is listed, while Table 6 presents information about the surface equipment. Prior to analysis, the dataset underwent rigorous cleaning and pre-processing to eliminate any outliers or missing values, ensuring the accuracy and reliability of the data used in the study.

Table 1 Input data

Parameter	Pres [bar]	Pbh [bar]	Pwh [bar]	Psep [bar]	Qg [m³/day]	Qf [m/day]
Input data	90.4	87	65	7.3	9191	0.1
Model results	91	86.8	65	7.3	9115	0.099

Table 2 PVT data

Serial number	Components	Unit of measure	Value
1.	Methane	mol %	95.30
2.	Ethane	mol %	0.26
3.	Propane	mol %	0.06
4.	Isobutane	mol %	0.00
5.	Butane	mol %	0.02
6.	Isopentane	mol %	0.00
7.	Pentane	mol %	0.00
8.	Hexane	mol %	0.09
9.	Nitrogen	mol %	3.45
10.	Carbon Dioxide	mol %	0.82
11.	Average molecular weight	g/mol	16.81
12.	Density relative to air	/	0.5813
13.	Density	kg/m^3	0.7123
14.	Wobbe's index (bottom)	MJ/m^3	43.02
15.	Lower heating value	MJ/m^3	32.80

Table 3 HD measurements

Depth	PRESSURE (kPa) – LEVEL (m)	
	Staircase	Dynamic
m	Dynamic	Grad.
3	kPa	kPa/m
0	6518	
100	6730	2,12
200	6980	2,50
300	7249	2,69
400	7495	2,46
500	7748	2,53
600	7967	2,19
700	8193	2,26
750	8316	2,46
800	8430	2,28
865	8588	2,43

Table 4 Data on production equipment

	Data on production equipment			
1	Inside diameter of column	127,3	*[mm]*	
2	Column outer diameter	139,7	*[mm]*	
3	Column section length	1239,5	*[m]*	
4	Column grade	H-40		
5	Tubing inner diameter	50,7	*[mm]*	
6	Tubing outer diameter	60,3	*[mm]*	
7	Tubing section length	858,7	*[m]*	
8	Tubing grade	J-55		
9	Packer installation depth	859,98	*[m]*	
10	Special equipment (description, characteristics, installation depth)	✓		
11	Perforation top	925	*[m]*	
12	Perforated interval length	1,5	*[m]*	
13	Inclinometer data	✓		
14	Geothermal gradient	X	[°C/m]	Not necessary, preferred

Table 5 Surface equipment data

	Data on surface equipment			
1	Pipeline length	420	*[m]*	
2	Internal diameter of the pipeline	73	*[mm]*	
3	Pipe wall thickness	5,2	*[mm]*	
4	Coefficient of thermal conductivity of pipelines	X	*[W/mK]*	
5	Absolute roughness of the inner wall of the pipeline	X	*[mm]*	
6	Average digging depth	0,8 - 1 m	*[m]*	
7	Soil temperature at the depth of burial	X	*[°C]*	
8	Thermal conductivity coefficient of the soil	X	*[W/mK]*	
9	Thermal conductivity coefficient of polyurethane foam insulation	X	*[W/mK]*	
10	Separator pressure	44	*[kPa]*	the well works through high pressure
11	Separator temperature	X	*[°C]*	

3.2 Creating and matching the model

NODAL analysis, as utilized in this study to model the well's performance (Mach et al. 1979), is a crucial technique in the realm of oil and gas reservoir engineering. It can be described as a systematic and comprehensive approach to assessing and optimizing the functionality of oil and gas wells, spanning from the reservoir to the wellhead. This analytical method considers various parameters such as wellbore configuration, tubing size, casing, and completion details, faithfully representing the intricacies of the actual well conditions.

The application of nodal analysis as the primary methodology in this study attests to its efficacy in understanding and predicting well behavior. By employing nodal analysis, researchers can identify and analyze the myriad factors that influence well performance, offering valuable insights into how the well is expected to behave under diverse scenarios. This method provides a holistic perspective on the entire well system,

allowing for precise predictions and targeted optimizations to enhance overall performance.

In the context of the oil and gas industry, IPR (Inflow Performance Relationship) and VLP (Vertical Lift Performance) are crucial concepts in the analysis of well performance. IPR represents the relationship between the production rate of a well and the flowing bottomhole pressure. Understanding IPR is essential for optimizing production and managing reservoir performance. On the other hand, VLP is concerned with the relationship between the production rate and the tubing head pressure, focusing on the efficiency of artificial lift systems (Golan & Whitson, 1991).

The formulation used to describe surface liquid production rates and wellbore flowing pressure is referred to as the Inflow Performance Relationship (IPR). This concept has been extensively employed since the advent of bottom hole gauges in the 1920s. The simplest equation within the IPR framework is the Productivity Index. This index signifies the ratio of the total liquid surface flowrate to the pressure drawdown at the midpoint of the producing intervals and is expressed in Equation 1 (Golan & Whitson, 1991).

$$J = \frac{Q}{Pr - Pwf} \tag{1}$$

Where:

J – Productivity index, $m^3/d/bar$

Q- Surface flowrate at standard conditions, m^3/d

Pr – Static bottom hole pressure, bar

Pwf – Flowing bottom hole pressure, bar

From Eq. 2 surface flowrate at standard conditions is defined as:

$$Q = J\,(Pr - Pwf) \tag{2}$$

In a great number of mature wells there are no downhole pressure gauges installed and flowing bottom hole pressure can be estimated from Eq. 3 (Boxer, 1988).

$$Pwf = Pc + \left(\frac{\rho \cdot g \cdot H}{1000}\right) \tag{3}$$

Where:

Pc – Casing pressure, bar

ρ – Density of liquid, kg/m^3

g – Acceleration of gravity, value 9,81 m/s^2

H – Height of fluid column, m

Vogel gives the second available method in Eq. 4 (Vogel, 1968).

$$Q = Q_b + (Q_{max} - Q_b)(1 - 0.2\,\frac{Pwf}{Pb} - 0.8\,\frac{P_{wf}^2}{P_b^2}) \tag{4}$$

Where:

Q – Production rate, m^3/d

Pb – Bubble point pressure, bar

Qmax – Maximum vogel rate, m^3/d

Qb – Measured rate at bubble point, m^3/d

Maximum Vogel rate is given in Eq. 5.

$$Q_{max} = \frac{P_b \cdot J}{1.8} \tag{5}$$

And in Eq. 6 is given rate measured at bubble point.

$$Q_b = J\,(P_{r-} P_b) \tag{6}$$

Therefore, the productivity index by Vogel is given in Eq. 7.

$$J = \frac{Q}{\left((Pr - Pb) + \frac{Pb\,(1 - 0.2\frac{P_{wf}}{P_b} - 0.8\frac{P_{wf}^2}{P_b^2})}{1.8}\right)} \tag{7}$$

The relation indicates that for each pressure decreasing on the bottom of drawdown or relief of formation backpressure against the face of the formation, result will be increase in production rate. Casing pressure have significant effect on production rate (Martinovic, 2022).

Vertical Lift Performance (VLP) correlations are empirical relationships or mathematical expressions that help predict and analyze the performance of artificial lift

systems in oil and gas wells. These correlations are essential tools for engineers and practitioners in the industry to estimate production rates, optimize lift systems, and make informed decisions about well operations.

The Gray Vertical Flow correlation, developed by H. E. Gray from Shell Oil Company, is employed to analyze pressure loss and holdup in vertical gas and condensate systems, where the predominant phase is gas. This correlation treats the flow as single-phase, assuming that any separated water or condensate adheres to the pipe wall. The applicability of this correlation is observed in vertical flow scenarios characterized by velocities below 15.24 m/s., tube sizes below 88.9mm, condensate ratios below 225 m^3/d, and water ratios below 8 m^3/d (Pipesim, 2017).

The creation of a well model during NODAL analyses consists of the following steps:

1. Input Well completion details: Enter completion details such as tubing size, casing size, completion type, and any artificial lift methods if applicable.
2. PVT Properties: Define the PVT properties for the well fluids. Input information such as fluid composition, density, viscosity, and other relevant properties. This data is crucial for accurate fluid flow calculations.
3. Define Well Inflow Performance Relationship (IPR): Establish the relationship between wellbore pressure and production rate. This is crucial for predicting well productivity under various conditions.
4. Definition of Hydrodynamic Measurements: Data from the results of the last relevant measurements of dynamic pressure profiles in the well are entered.
5. Vertical Lift Performance (VLP): Set up Vertical Lift Performance (VLP) models, that involve defining the well's response to changes in tubing and casing pressures.
6. Run Nodal Analysis: Execute the nodal analysis to simulate the well's behavior under the specified conditions. PipeSim will calculate pressures, temperatures, and flow rates at different points in the well and production system.
7. Review Results: Analyze the simulation results, focusing on parameters such as wellhead pressure, tubing and casing pressures, flow rates, and temperature profiles. Evaluate the well's performance under different operating conditions.
8. Optimization: If necessary, adjust parameters such as choke size, completion design, or artificial lift settings to optimize well performance.

3.3 Sensitivity Analysis

A sensitivity analysis was conducted post the development and validation of the well model. This analysis aimed to examine the impact of various operational parameters on hydrate formation, focusing specifically on choke positions, methanol injection rates and separator pressure.

The main goal of these analyses is to find the optimal solution for preventing hydrate formation and ensuring stable production. Additionally, this type of analysis allows us to compare different approaches to addressing the issue and evaluate their impact on well behavior.

Choke Position Analysis: Different choke positions were simulated, and their impact on the well's pressure and temperature profiles were analyzed. These profiles are crucial in understanding the conditions under which hydrates form. By changing the choke position, a sudden drop in pressure is facilitated under different temperature conditions, reducing the likelihood of hydrate formation. By varying the choke depth from the wellhead towards the bottom, every 50 meters, the shallowest installation point will be determined to ensure stable operation.

Methanol Injection Analysis: The study also simulated various rates of methanol injection to evaluate their effectiveness in preventing hydrate formation. Methanol, serving as a thermodynamic inhibitor, lowers the temperature at which hydrates form, mitigating the risk associated with their formation. The main goal of the analysis is to determine the exact position for injecting hydrate inhibitors and to identify the minimum quantity of chemical required to prevent hydrate formation, aiming to optimize operational production costs. The precise injection point will be determined through the analysis of hydrate formation risk graphs, and the injection point will be placed immediately before the hydrate formation risk zone. Following that, by varying the daily amount of injected methanol, the minimum sufficient quantity will be determined.

Changing the separator pressure: One of the methods to prevent hydrate formation is changing the separator pressure. This involves transferring the well from a low-pressure separator to a high-pressure separator, provided that the aboveground infrastructure allows for it. In the case of this well, the transfer from a separator pressure of 5 bars to a separator pressure of 43 bars will be analyzed. Such a change reduces the pressure drop across the choke, decreasing the likelihood of hydrate formation.

4 RESULTS AND DISCUSSION

Based on the analysis of the production profile, it can be concluded that the well casing is hermetic, and the well produces a very small quantity of fluid, approximately 0.1 m^3/d. During the monitored period, there were two choke size changes, from 3 mm to 3.3 mm at the end of June and from 3.3 mm to 3.5 mm in mid-July, both accompanied by an increase in production. Between November 25th and December 15th, a sudden tubing pressure spike was observed, coinciding with a production decline. As there was no corresponding increase in line pressure and considering external temperatures during that time of the year, it is concluded that hydrate deposits are forming. Production stabilizes after pipeline cleaning. Subsequent regular methanol dosing prevents the formation of significant deposits and production decline. In September, the well is switched from a

low-pressure separator to a high-pressure separator, leading to a reduction in choke pressure drop and a decreased likelihood of hydrate formation.

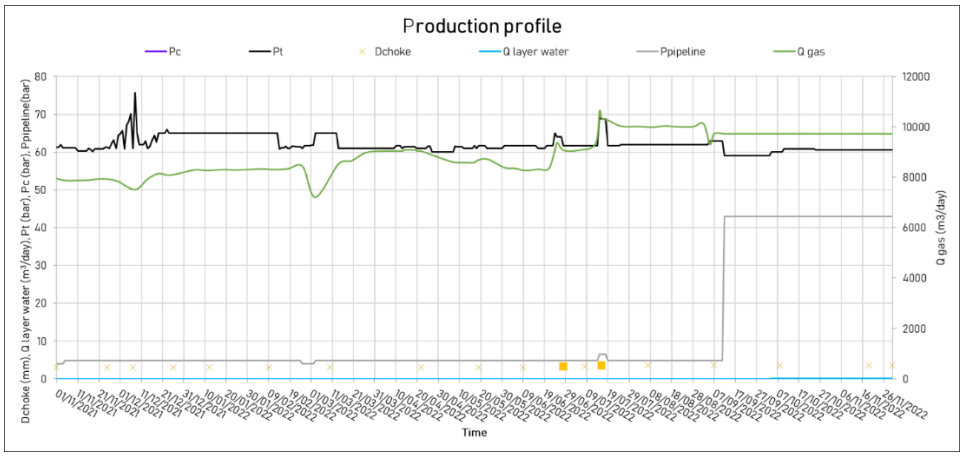

Figure 1 Production profile

In Figure 2, a wellbore sketch generated in Pipesim is presented based on the downhole production equipment data from Table 4. Additionally, the nodal point at the bottom of the well at a depth of 912 m is depicted in the figure. Figure 3 illustrates the surface infrastructure and the position of the upper nodal point located at the wellhead.

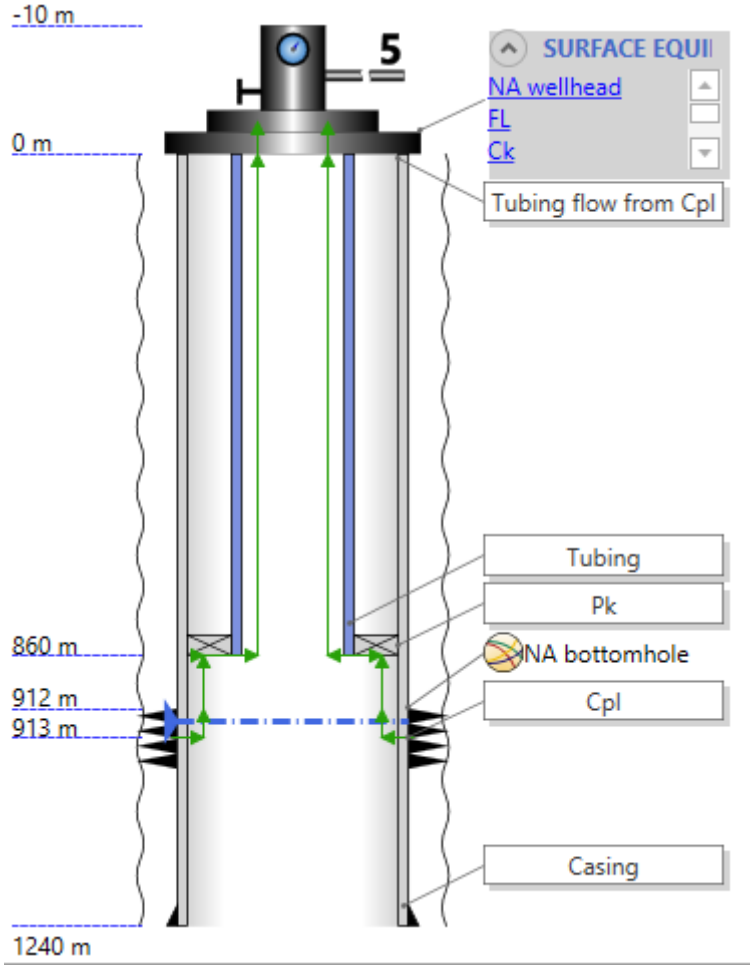

Figure 2 Sketch of well

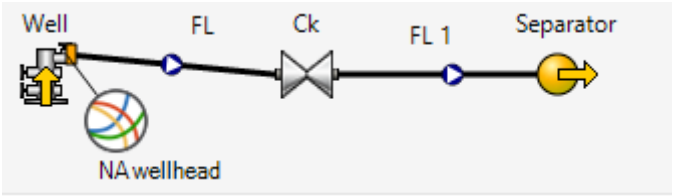

Figure 3 Surface equipment

As the next step in solving the given business case, following the establishment of the wellbore construction and characterization of the fluid, production and pressure were imposed at both nodal points (bottomhole and wellhead NAs) based on available production data and results of hydrodynamic measurements. Subsequently, in the

continuation of the scientific paper, the solution at the bottom of the wellbore (Fig. 4) and the solution at the wellhead (Fig. 5) are presented. Vertical Lift Performance (VLP) is described by the Gray (Gray 1974) correlation, while fluid inflow from the reservoir is simulated using the PI method (Craft 1959).

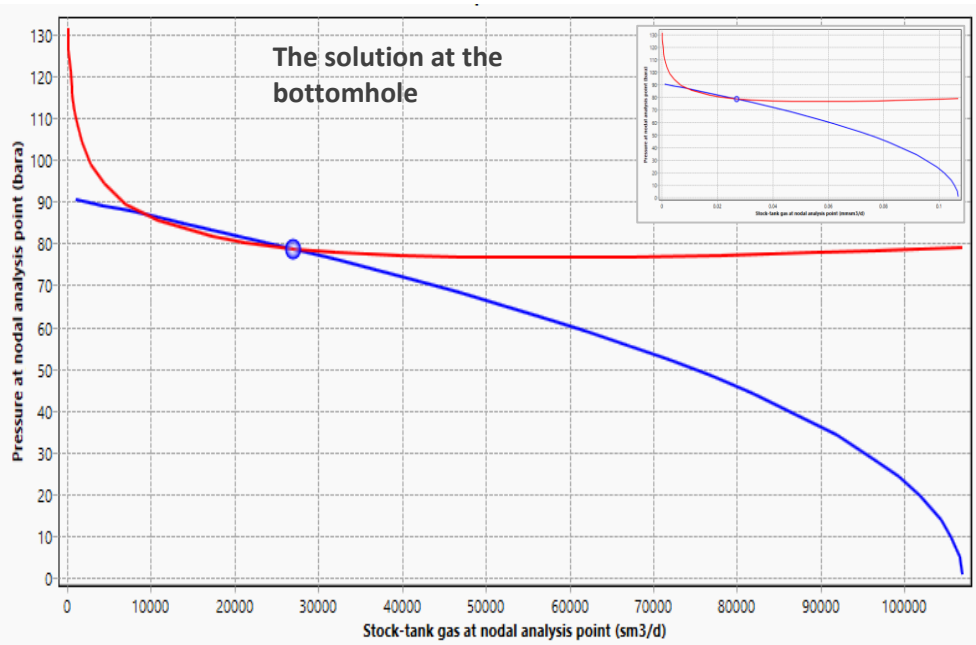

Figure 4 Nodal point at the bottom

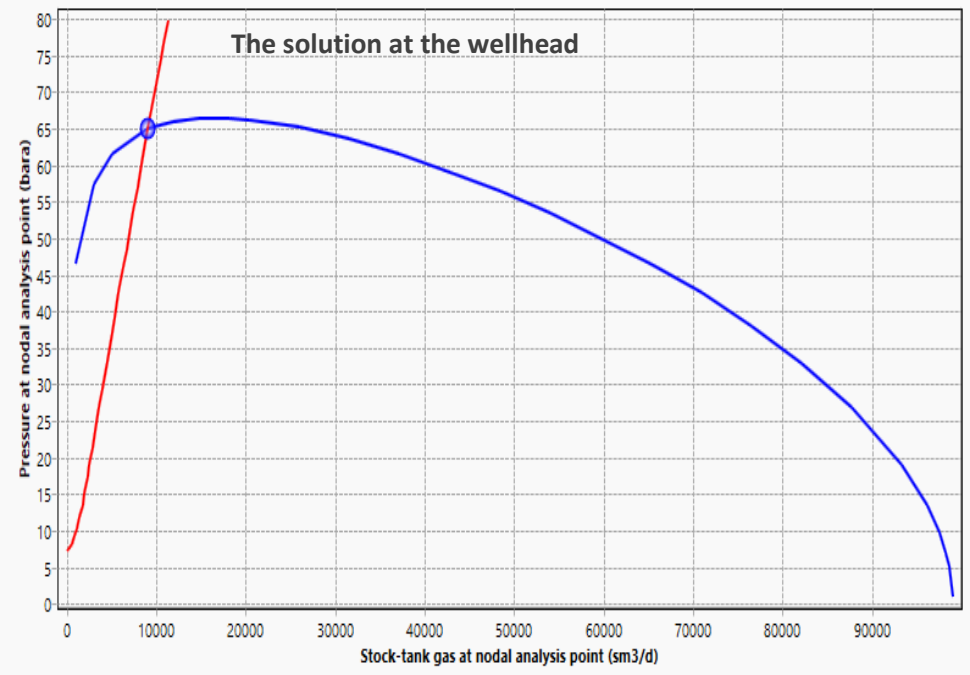

Figure 5 Nodal point at the head

By comparing the results of the baseline model presented in Fig. 4 and Fig. 5 with the input production data from Table 1 (outlined above in the paper), it can be concluded that the model is fitting well, i.e., the well model completely describes the current state of the well, and further analyses can be conducted based on its behavior.

Based on the constructed phase diagram for this well (Fig. 6), an analysis of the hydrate line reveals the potential for hydrate formation within the operational production parameters of pressure and temperature. It is precisely for this reason that we can assert that a thorough analysis of this issue is necessary for this well.

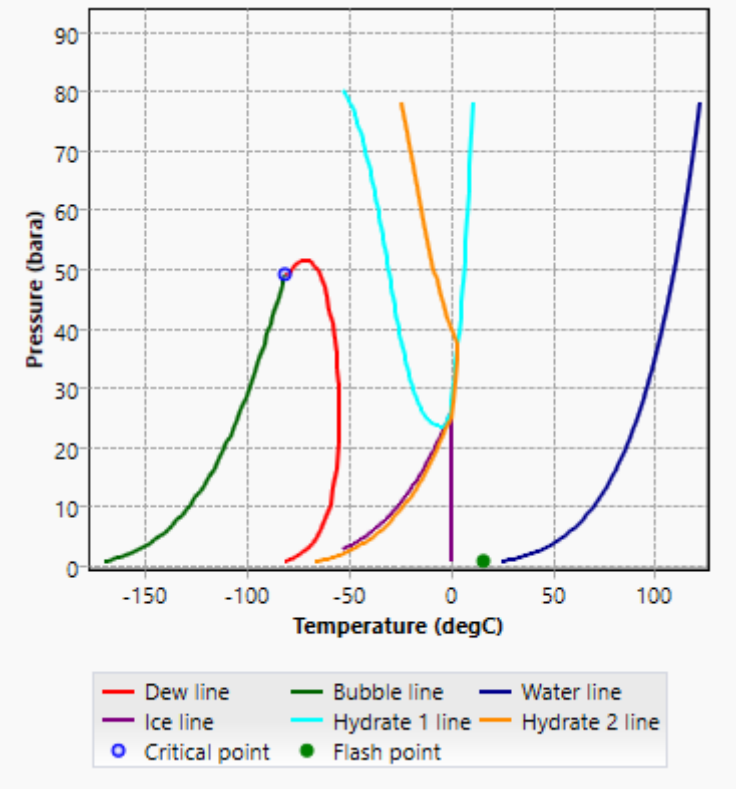

Figure 6 Phase diagram

Hydrate formation risk

In the baseline model, a hydrate formation risk analysis was conducted. Conditions for hydrate formation were tested under ambient temperatures around the wellhead of 5°C, which is the case during winter months in the area where the well is located. Based on the test results (Fig. 7), it is observed that around the wellhead, specifically at the choke (912 m), there is a risk of hydrate formation as the hydrate sub-cooling delta temperature value is above 0°C. From the analysis, it can be concluded that there is no risk in the wellbore column and in the pipeline after the surface choke. In the temperature profile (Fig. 8), it can be seen that in the wellbore, the temperature gradually decreases from the bottom temperature of 60°C to 9°C, which is the temperature of the fluid at the wellhead. At the choke installation point, there is a sudden temperature jump to 18°C, followed by a rapid decrease to -15°C, promoting hydrate formation.

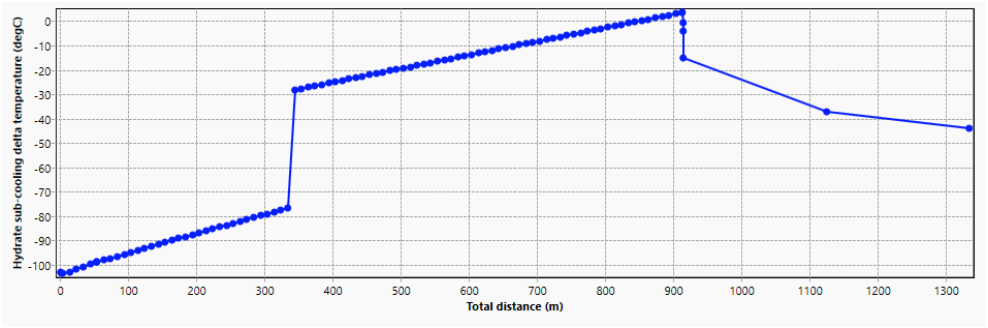

Figure 7 Risk of hydrate formation

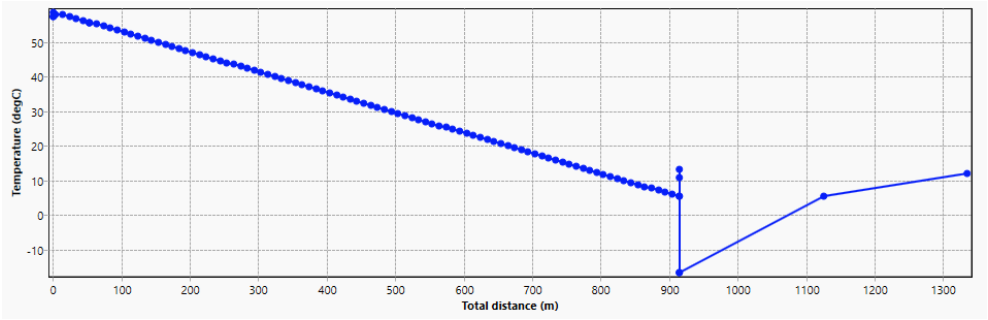

Figure 8 Temperature profile of the wellbore

Installation of a downhole choke

One of the tests conducted in the model to find an optimal solution for the hydrate formation challenge is the installation of a downhole choke. The goal of the performed sensitivity analyses is to determine the minimum installation depth, thus reducing operational costs associated with equipment manipulation.

The first test involved installing the choke at a depth of 50 meters from the wellhead, as illustrated in the diagram below (Fig. 9). Based on the obtained values of hydrate sub-cooling delta temperature, it can be concluded that the chosen depth is insufficient to prevent hydrate formation (Fig. 10).

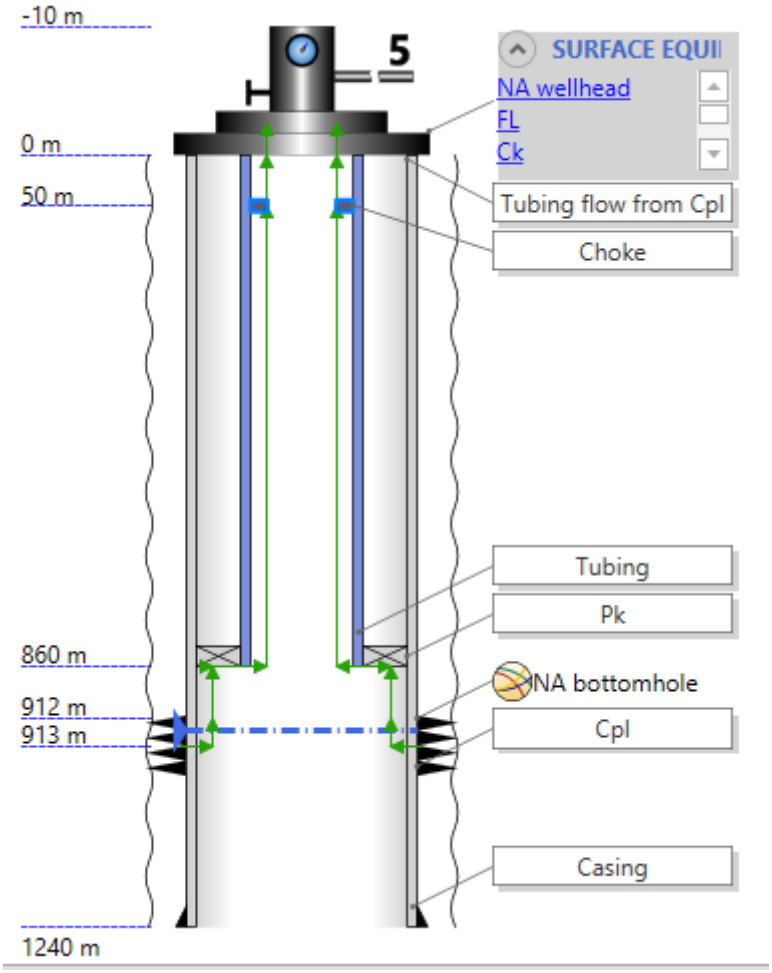

Figure 9 Well construction with a downhole choke at a depth of 50 m

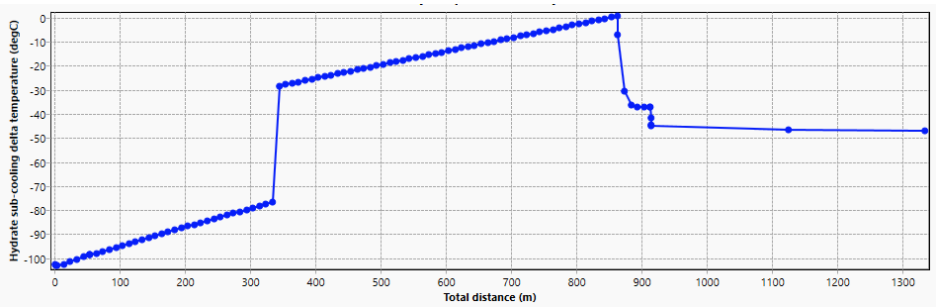

Figure 10 The risk of hydrate formation at a choke installation depth of 50 meters

The next test was conducted by installing the choke at a depth of 100 meters from the wellhead (Fig. 11). A nodal analysis was performed, and based on the results of the hydrate sub-cooling delta temperature (Fig. 12), it was concluded that the installation depth is sufficient to prevent hydrate formation throughout the system: reservoir-wellbore-pipeline-separator, even under winter conditions when the ground temperature around the wellhead is approximately 5°C.

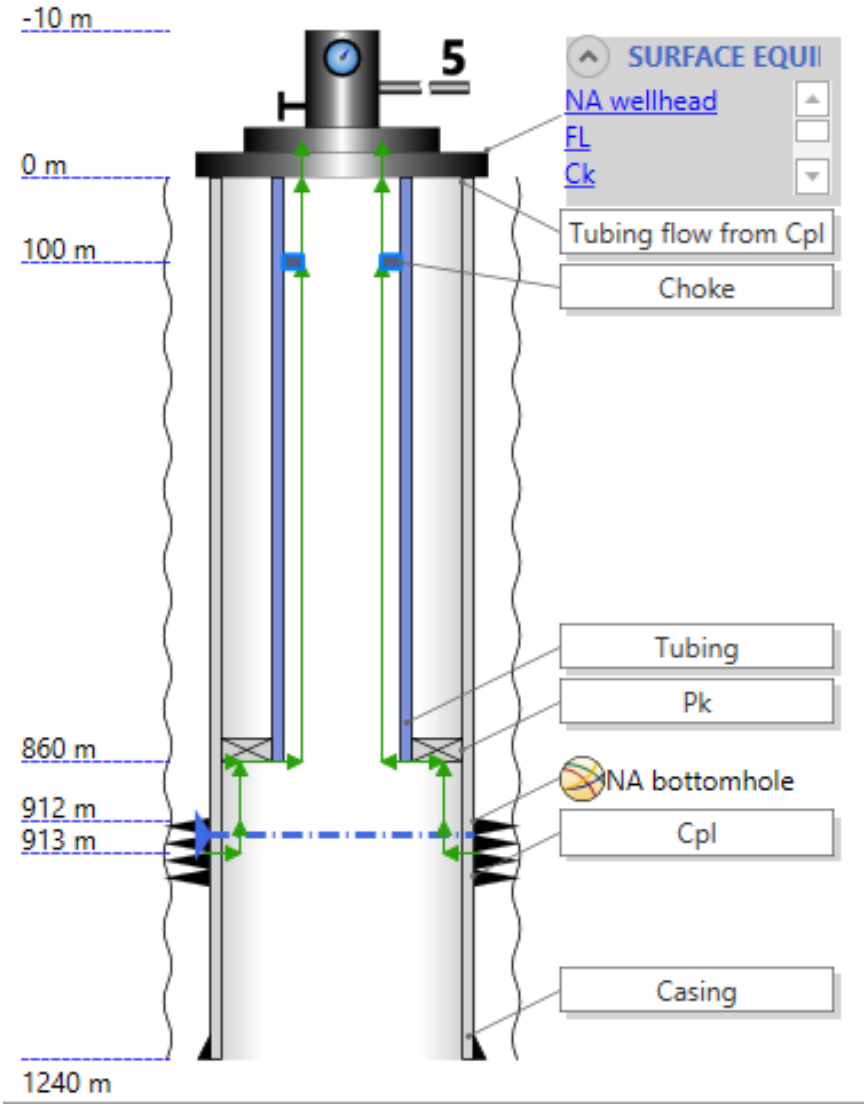

Figure 11 Well construction with a downhole choke at a depth of 100 m

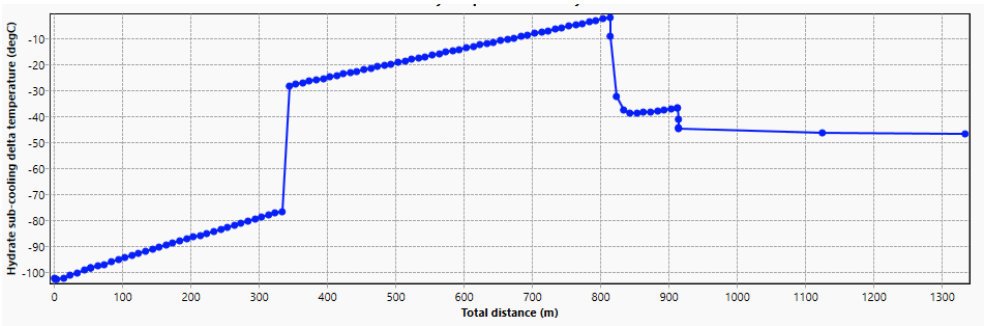

Figure 12 The risk of hydrate formation at a choke installation depth of 100 meters

Methanol dosing

The next method of combat simulated in the model is the continuous dosing of methanol using a dosing pump. This method chemically prevents the formation of hydrate plugs.

The first test involved placing the injection point immediately after the wellhead and before the surface choke located at the location (Fig. 13). A sensitivity analysis of hydrate formation was conducted with different amounts of dosed methanol (Fig. 14). Based on the results, it can be concluded that regardless of the dosed quantity, the problem cannot be solved with the surface injection point alone, as the hydrate sub-cooling delta temperature at the wellhead exceeds 0°C.

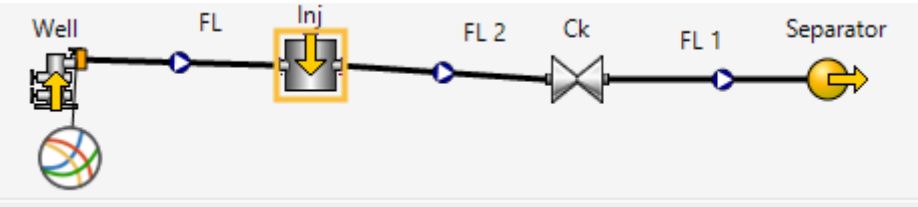

Figure 13 Infrastructure with the methanol injection point in place

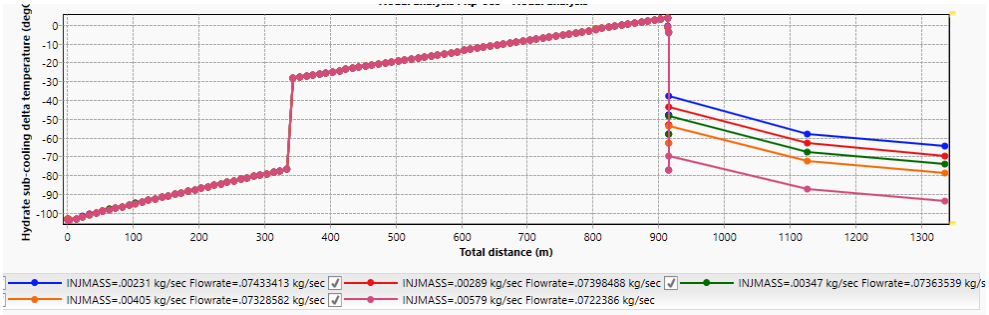

Figure 14 The probability of hydrate formation at different amounts of dosed methanol

In the upcoming test, the dosing point is set 100 m from the wellhead (Fig. 15), achievable through capillary dosing of the inhibitor. Through the analysis of the minimum effective dose, it has been determined that at a dosing rate of 10 kg/d of methanol, the well is at the threshold of hydrate formation. However, at a dosing rate of 30 kg/d, sufficient protection against hydrate formation is ensured (Fig. 16).

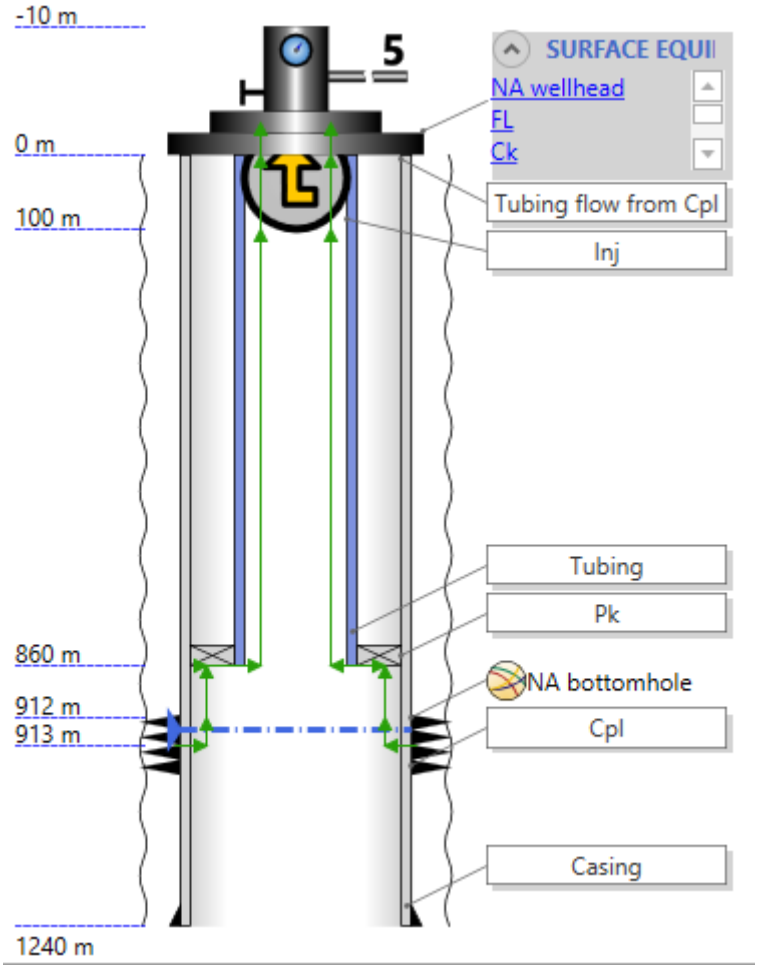

Figure 15 Well construction with the methanol injection point set at 100 m

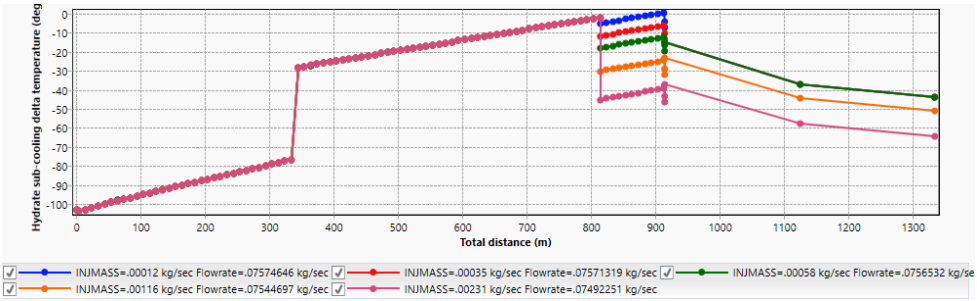

Figure 16 The probability of hydrate formation at different amounts of dosed methanol

At a chemical dosing depth of 200 m (Fig. 17), regardless of the amount of methanol, the necessary protection against paraffin precipitation is ensured (Fig. 18). However, increasing the dosing depth leads to higher operational costs and complicates the equipment installation process.

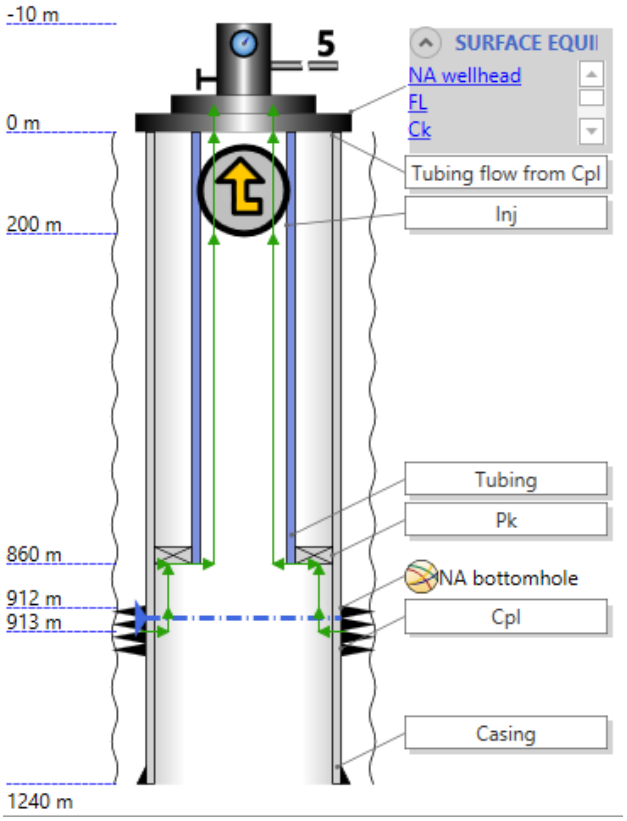

Figure 17 Well construction with the methanol injection point set at 200 m

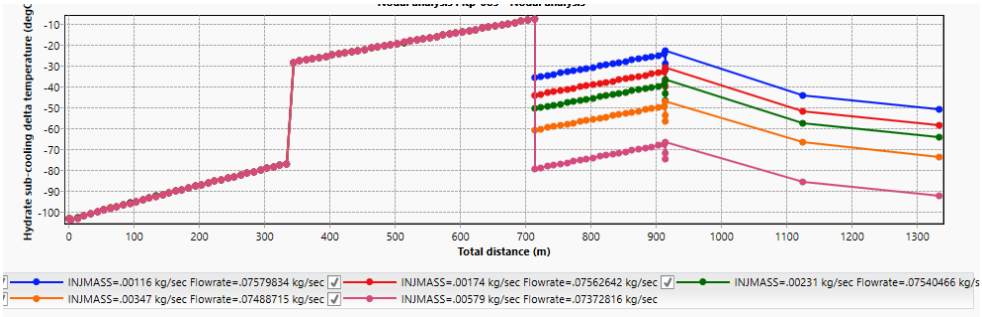

Figure 18 The probability of hydrate formation at different amounts of dosed methanol

Well transfer to a high-pressure separator

One of the methods to combat this is to transfer the well from a low-pressure separator to a high-pressure separator, which has been implemented in this well. During the change in separator pressure from 7 bar to 43 bar, there is a slight pressure increase at the wellhead by several bars, and the production decreases by almost 2000 m3/d. This can be compensated by increasing the choke diameter. The results of nodal analysis during the change in separator pressure are presented below in the paper – the solution at the bottomhole nodal point (Fig. 19) and the solution at the wellhead nodal point (Fig. 20). However, the analysis of the probability of hydrate formation shows that this measure is not sufficient to address the issue in winter months and can only be applied in conditions where the ambient temperature is above 10°C (Fig. 21).

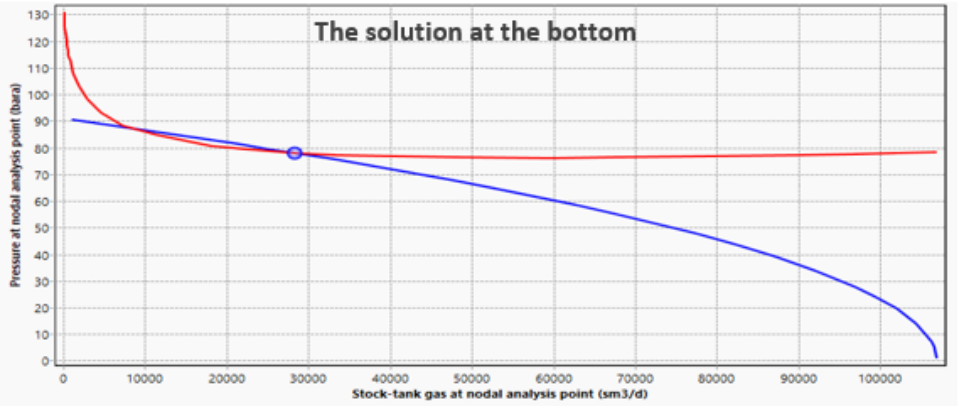

Figure 19 Well model at high pressure translation – nodal point at the bottom

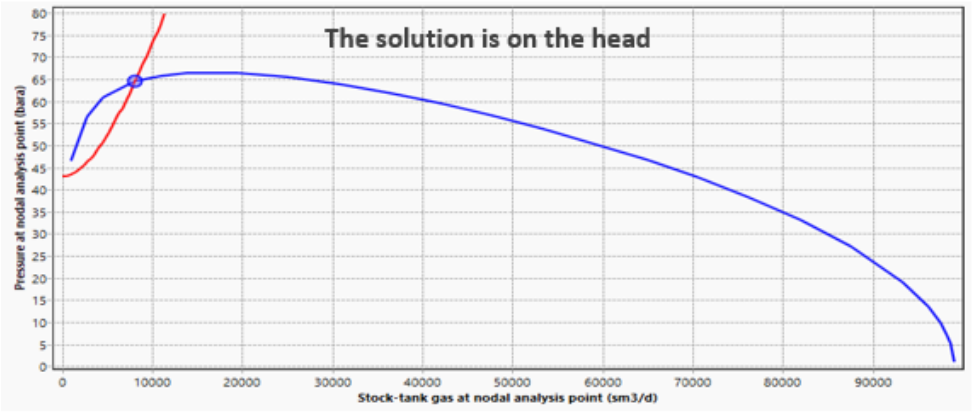

Figure 20 Well model at high pressure translation – nodal point at the wellhead

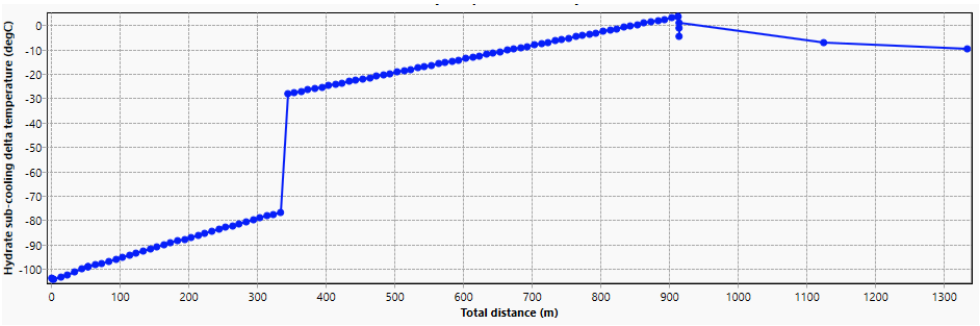

Figure 21 The probability of hydrate formation after transferring the well to a high-pressure separator

5 CONCLUSION

The issue of hydrate formation is a common challenge in the exploitation of gas wells, making it a perpetually relevant subject. While there are several approaches to addressing this problem, it is essential to individually assess each case and each well. Nodal analysis and the development of well modeling software have made it possible to do so. Currently, modeling is an indispensable tool for engineers in defining measures and recommendations for preventing hydrate formation, both in pipelines and tubing wells.

This paper presents a methodological approach to the analysis and resolution of the problem using a specific well as an example. Three methodologies and their effectiveness in the specific case were analyzed – installing a downhole choke, dosing methanol, and transferring the well from a low-pressure separator to a high-pressure separator.

Based on sensitivity analyses conducted on the well model, it was concluded that preventing hydrate formation by installing a downhole choke at a depth of 100 m from the wellhead is possible. Dosing methanol at the surface before the nozzle is not effective in preventing hydrate formation due to a rapid temperature drop at the wellhead. In the case of methanol dosing and combating the problem using this chemical method, it is necessary to dose the chemical at a depth of 100 m through capillary dosing at a rate of 30 kg/d. In this specific case, transferring to a high-pressure separator is not a sufficiently effective method for application in the winter period when the ambient temperature is below 5°C.

Considering all the presented information and the results of all conducted analyses, the author's recommendation is to install a downhole choke at a depth of 100 m, which is economically more viable than capillary methanol dosing. This approach also allows for the prevention of hydrate formation.

It's important to note that during the workover for installing a downhole choke, there are one-time installation costs if a choke seat already exists. If not, workover is required, including installation of both the seat and the choke. On the other hand, with methanol dosing, there are capital investments for dozing pump, workover for the installation of capillary pipes, and ongoing operational costs related to methanol consumption.

REFERENCES

ALEMI, M., JALALIFAR, H., KAMALI, G.R. AND KALBASI, M. (2011) 'A mathematical estimation for artificial lift systems selection based on ELECTRE model', Journal of Petroleum Science and Engineering, Vol. 78, No. 1, pp. 193–200.

BOXER G. (1988) Hydrostatic Pressure. In: Fluid Mechanics. Macmillan Work Out Series. Palgrave, London.

CRAFT, B. C., AND MURRAY F. HAWKINS. (1959) Applied petroleum reservoir engineering

DUAN, X., ZUO, J., LI, J., TIAN, Y., ZHU, C., & GONG, L. (2023) Prediction of gas hydrate formation in the Wellbore. Energies, 16(14), 5579. https://doi.org/10.3390/en16145579

Gas hydrate control. (2015) In Elsevier eBooks (pp. 405–443). https://doi.org/10.1016/b978-0-12-803734-8.00013-8

GOLAN MICHAEL, WHITSON H. CURTIS "Well Performance 2nd Edition", Department of Petroleum Technology and Applied Geophysics, Norwegian University of Science and Technology, 1995.

GRAY, H. E. (1974) "Vertical Flow Correlation in Gas Wells". User manual for API 14B, Subsurface controlled safety valve sizing computer program. API.

HASHEMI, H., BABAEE, S., TUMBA, K., MOHAMMADI, A. H., NAIDOO, P., & RAMJUGERNATH, D. (2019) Experimental study and modeling of the kinetics of gas hydrate formation for acetylene, ethylene, propane and propylene in the presence and absence of SDS. Petroleum Science and Technology, 37(5), 506–512. https://doi.org/10.1080/10916466.2018.1531024

MACH, J., PROANO, E., AND BROWN, K.E. (1979) A Nodal Approach for Applying Systems Analysis to the Flowing and Artificial Lift Oil or Gas Well. Paper SPE 8025 available from SPE, Richardson, Texas.

MAKOGON, Y F. (1997) Hydrates of hydrocarbons. United States: N. p., 1997. Web.

MARTINOVIC, B., DANILOVIĆ, D., GRUBAC, B., & FADIGA, R. (2022) Productivity improvement with use of beam gas compressor: pilot test in Southeastern Europe mature field. International Journal of Oil, Gas and Coal Technology, 30(1), 46.

МУСАКАЕВ, Н. Г., BORODIN, S. L., & KHASANO, M. K. (2021) Numerical modeling of gas hydrate formation in a porous collector. PMTF. Prikladnaâ Mehanika, Tehničeskaâ Fizika, 62(4), 57–67. https://doi.org/10.15372/pmtf20210406

NWANKWO, K. O. (2019) 'Gas Production Optimization Using Thermodynamics Hydrate Inhibition Flow Assurance Method', SPE-198842-MS, Society of Petroleum Engineers. Presented at the Nigeria Annual International Conference and Exhibition, Lagos, Nigeria, 5–7 August 2019.

PING, X., HAN, G., CEN, X., BAI, Z., ZHU, W., PENG, L., & MA, B. (2022) Prediction of Pressure and Temperature Profiles and Hydrate Formation Region in ESP-Lifted Natural Gas Hydrate Wells. SPE Western Regional Meeting. https://doi.org/10.2118/209288-ms

PIPESIM Version 2017.2 User Guide. PIPESIM User Guide. Copyright © 2017 Schlumberger

SHUKLA, P. K., SINGHA, D. K., & SAIN, K. (2022) Modeling of in-situ horizontal stresses and orientation of maximum horizhontal stress in the gas hydrate-bearing sediments of the Mahanadi offshore basin, India. Geomechanics and Geophysics for Geo-Energy and Geo-Resources, 8(3). https://doi.org/10.1007/s40948-022-00401-6

SLOAN E. D. (2010) Natural Gas Hydrates in Flow Assurance; Gulf Professional Publishing, 2010.

SONG, G., LI, Y., & SUM, A. K. (2020) Characterization of the coupling between gas hydrate formation and multiphase flow conditions. Journal of Natural Gas Science and Engineering, 83, 103567. https://doi.org/10.1016/j.jngse.2020.103567

STRAUME, ERLEND & KAKITANI, CELINA & MORALES, RIGOBERTO & SUM, AMADEU. (2016) Study of Gas Hydrate Formation and Deposition Mechanisms in Hydrocarbon Systems. 10.26678/ABCM.ENCIT2016.CIT2016-0255.

WANG, H., DIAO, H., TAN, X., JIANG, D., CHEN, Y., LI, Z., GAN, B., & ZOU, F. (2022) Study on Hydrate Formation in Deep-Water Gas Well Intervention Operation. In Advances in transdisciplinary engineering. https://doi.org/10.3233/atde220397

WEI, NA, et al. (2021) "Risk Prediction of Non-equilibrium Formation of Natural Gas Hydrate in the Wellbore of a Marine Gas/Water-producing Well." Natural Gas Industry B 8, no. 1 88-97.

UNDERGROUND MINING ENGINEERING 43 (2023) 71-78 UDK 62
UNIVERSITY OF BELGRADE - FACULTY OF MINING AND GEOLOGY ISSN 03542904

Original scientific paper

INFLUENCE OF NATURAL MINERALS ON CONTAMINATED SOLUTIONS pH VALUES

Mirko Grubišić[1], Nataša Đorđević[1], Slavica Mihajlović[1]

Received: March 27, 2023 **Accepted:** April 11, 2023

Abstract:

The protection and arrangement of agricultural areas in order to obtain health-safe food is extremely important to know the mobility of heavy metals lead, cadmium, zinc and uranium as radionuclides. This research investigated the influence of mineral raw materials (apatite and zeolite) on the mobility of heavy metals and radionuclides in a column system with constant pressure at different pH values (5.0 and 7.0). The tested solutions were contaminated with metals (lead, cadmium, zinc and uranium), in a concentration of 300 mg/l in time intervals of 30, 60, 90, 120 and 180 minutes. It was experimentally determined that there were significant changes in the pH value of the filtrate. The results showed that both apatite and zeolite successfully immobilized lead at both pH values. Uranium immobilization was better performed in columns with apatite, zeolite showed better properties in cadmium immobilization, and tests on a solution contaminated with zinc showed that both apatite and zeolite show similar affinity. The obtained results were statistically processed using the method of two-factor analysis of variance with repeated measurements. Further research will be based on monitoring the morphophysiological properties of underground and aboveground parts of plants on contaminated soil samples when apatite and zeolite are applied.

Keywords: pH value, natural minerals, contamination, influence

1 INTRODUCTION

Environmental pollution, especially the land on which crops are used for food grow, was a consequence of technological development, especially in the last 70 years. Due to the increasing number of inhabitants, there was an increased request both for food and raw materials. This process inevitably led to the contamination of water, water, and land. New technologies and procedures have been developed in order to reduce the contamination of endangered soils, especially from heavy metals (Pb, Zn, Cd) and radionuclides (U). Due to the increased soil contamination, the process of assisted natural

[1] Institute for technology of nuclear and other mineral raw materials,
Franse d`Eperea 86, 11000 Beograd
E-mails: m.grubisic@itnms.ac.rs; n.djordjevic@itnms.ac.rs; s.mihajlovic@itnms.ac.rs

remediation was started with the technology of immobilizing heavy metals using natural materials and preventing the mobility of pollutants through complex soil system.

In the constructed column system with mineral raw materials-materials (zeolite, apatite), ion exchange and precipitation processes reduced the content of Pb, Zn, Cd and U contaminants in the filtrate compared to the base solution. According to Jain & Ram, (Jain, 1997) several factors influence these processes such as: mineral composition of the substrate-raw material-filter, filtration coefficient, porosity and pore size, pH value of the base solution, contaminant content.

2 LABORATORY RESEARCH

This first part of the laboratory research in the column system determined the changes in the pH value of the basic solutions of contaminants Pb, Cd, Zn, U (pH=5.00 and pH =7.00) after filtering through columns with zeolite and apatite. Monitoring of changes in the basic solution was performed in 5-time intervals (t1-t5), with the first four intervals (t1-t4) being 30 minutes apart and the t5 interval lasting 60 minutes. Tests in these pH environment conditions (pH 5.00 and pH 7.00) represent a similar model that occurs in the tested soils of the pseudogley and chernozem types because similar conditions of active acidity prevail (acidic, neutral), which is the subject of the second part of the research. Graph 1 shows the change in basic starting pH=5.00 of toxic solutions of Pb, Zn, Cd, U when passing through columns with zeolite and apatite.

Significant changes in the basic contaminated solution (pH 5.00) were observed, indicating ion exchange processes carried out in zeolite and apatite. The highest pH value of the output solution from the column (filtrate), at pH=5.00, was recorded by the basic solutions of Pb and U through the column filled with apatite in all time intervals, (t1-t5). Contaminated U solutions passed through the apatite column have minimal fluctuations in the pH of the filtrate (0.16), at pH =5.00, varying in a narrow range, 7.77-7.93. A slightly wider fluctuation of the pH value of the filtrate (0.18) through the apatite column was recorded in the Pb solution, 7.69-7.87, during the time interval of 180 minutes.

Such changes in pH value indicate the conclusion that the reactions of apatite with a contaminated solution of Pb and U and an acidic environment are very fast and stable, thanks to the sufficient amount of exchangeable carbonates present. As for the changes in the pH value of basic solutions (pH=5.00) contaminated with Zn, Cd, through the column filled with apatite, the values also record changes in the pH value of the solution, but of a slightly weaker intensity during the entire duration of the experiment of 180 minutes. Base contaminated solutions of Cd and Zn (pH =5.00) passed through the apatite column have lower filtrate pH values and record a linear, slight decrease in filtrate pH values for Zn (7.28-6.68) and slightly faster for Cd (7.11-6.15) over time. (t1-t5) of 180 minutes.

In the article by Knox et al. (Knox, 2003), the pH of the soil solution did not remain constant comparing the control and two mineral supplements (phillipsite, apatite). The pH value of the soil solution in the control variant was 3.84 (±0.01), in the variant with apatite it was 4.89 (±0.05) and for phillipsite it was 4.26 (±0.05). The increase in pH with mineral raw materials is probably the result of alkali action from the apatite, as a hint of the relatively high calcium carbonate content. The obtained results, at pH=5.00, indicate that good quality apatites were used and that they can have a wide and varied application, due to the speed and ability to react, because most phosphate-apatites are not good for soil remediation. For good results, the mineral raw material from the apatite group should: 1) have as much exchangeable carbonate as possible, 2) no fluorine in exchangeable form, 3) have traces of harmful metals in the initial structure, 4) be poorly crystalline or equally amorphous, and 5) has high internal porosity (Conca, 1997).

Changes in the pH value of basic contaminated (Pb, Zn, Cd, U) solutions, pH = 5.00, were also recorded after passing through the columns that were filled with zeolite, but at a much lower intensity. The range of new changes in the pH value of the base solution after passing through the zeolite columns ranges from pH = 5.15 for the Zn filtrate in the time period t5 to pH = 6.81 for the U filtrate in the time period t1. The largest oscillations of the pH value of the filtrate in the time interval t1-t5 on zeolites, at pH=5.00 of the basic solution, were recorded by the contaminated Cd solution (6.65-5.17), which decreased by 1.48 pH units. A similar tendency was also observed with the Cd solution (7.11-6.15) that was passed through the column with apatite, where the pH change was slightly lower, 0.96 pH units. New changes in the pH value of the basic contaminated solution (pH=5.00), after passing through the zeolite columns, have the same distribution of the influence of contaminants (U, Pb, Zn, Cd) as in the case of apatite. The biggest changes in pH value, between the basic solution and the filtrate solution, occurred in the solution with U, then Pb, and the least with Cd and Zn. This indicates the possibility of a great similarity between apatite and zeolite in the affinity towards certain toxic elements, regardless of the difference in the chemistry of their action (adsorption/precipitation).

The shown difference in the pH value of the initial solution and the filtrate solution, the dynamics of changes between mineral raw materials (apatite, zeolite) after treatment, occurred due to the composition, dynamics of receiving and the amount of adsorptive cautions that can influence such changes. It is known that the greatest affinity of apatite is for lead and uranium if they are found as contaminants, because they create stable complexes, precipitates. Apatite in its adsorptive complex has a slightly higher content of calcium, sodium and magnesium, which caused the newly created changes in pH value. The obtained results clearly indicate the affinity of certain mineral raw materials for toxic metals, as well as the degree and speed of possible success in establishing the dynamic balance of the adsorption or precipitation process. Graph 1 clearly shows the uniformity and stability of pH filtrate with Pb and U through the apatite column.

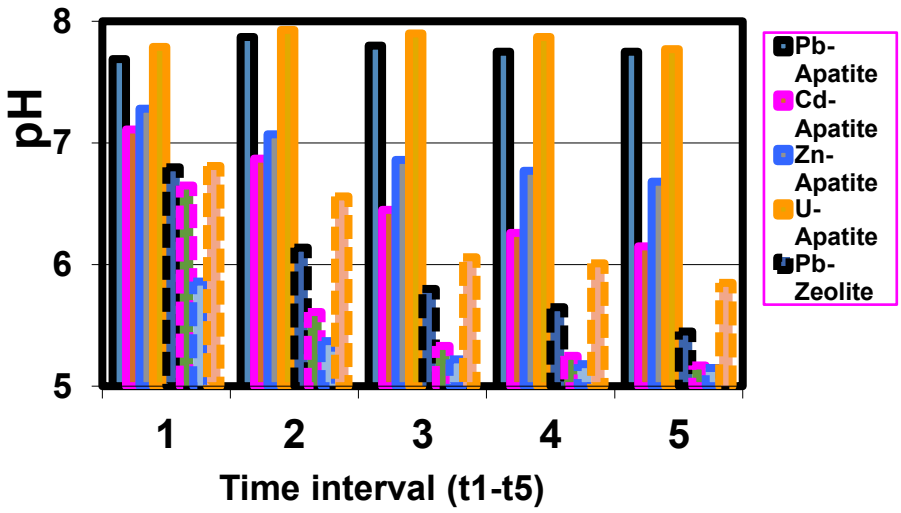

Graph. 1 Changes in the pH value of the basic solution pH = 5.00 after passing through columns with zeolite and apatite

Such a trend of uniformity was not established for the contaminants Zn and Cd (pH=5.00) by passing through apatite columns. Even greater oscillations in the time period (t1-t5) of 180 minutes, and lower differences compared to the base solution pH = 5.00 were recorded in the columns with zeolite, with the largest increases in the pH value of the filtrate compared to the base solution being recorded in the first two time intervals (t1-t2), in the first 60 minutes. Changes in the pH value of the filtrate of the solution with Pb, Zn, Cd and U also occurred when the basic contaminated solution, whose pH value was 7.00, was passed through the columns with zeolite and apatite (graph 2). The newly formed changes at pH value 7.00 are significantly less fluctuating compared to the base solution pH = 5.00, and the variations range from 6.77 to 7.96.

The same trend with the pH = 7.00 solution, that is, the biggest changes in the pH value, occurred as with the basic contaminated pH = 5.00 solution in the Pb and U filtrate obtained through the apatite column. The pH values of the filtrate are quite uniform with the apatite column for the contaminated solutions with Pb (7.70-7.94) and U (7.79-7.96).

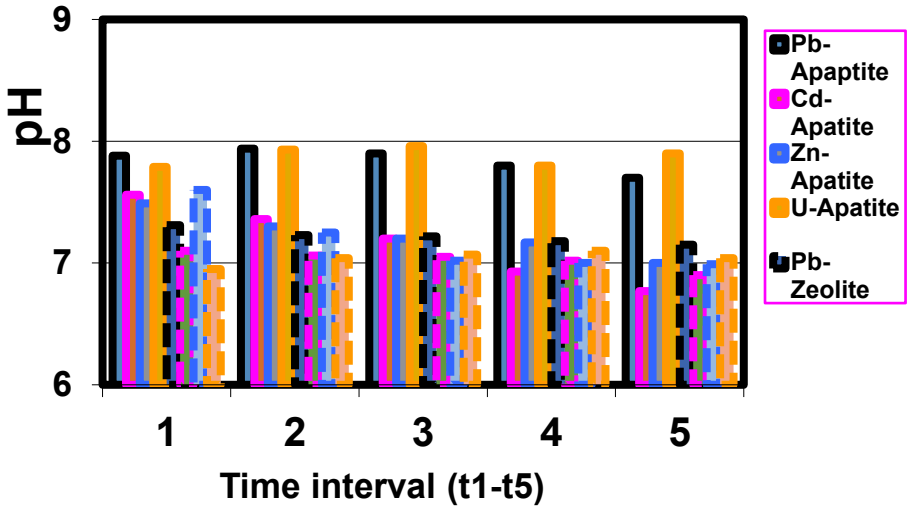

Graph. 2 Changes in the pH value of the solution for apatite and zeolite, after treatment with a toxic solution of pH 7.00

The resulting filtrate through apatites for Cd and Zn have a similar linear decrease in pH value in time t1-t5, for Cd from 7.56 to 6.77 and for Zn from 7.49 to 7.00. As with the basic contaminated solution pH =5.00, and in environmental conditions pH =7.00, the widest ratio of filtrate during time t1-t5 was recorded for Cd (0.79) and Zn (0.49) solutions.

Matusik et al. (Matusik, 2012) determined that hydroxy apatite affects the reduction of Cd content in the solution at different pH values of the basic solution 3, 5 and 7 and leads to an increase in the pH value of the basic solutions to 6.07, 6.90 and 7.21, respectively. In the experiment with natural apatite, the initial pH values were slightly changed to 3.59, 6.45 and 6.90. Such changes in the pH value of the solution can be explained by the influence of H^+ ions in the formation of different phosphate-anion species: HPO_4^{2-}, $H_2PO_4^-$ and H_3PO_4 (Manecki, 2000).

The zeolite-adsorbent, as a filter in the columns, affected the changes in the pH value of the basic contaminated solutions (Pb, Zn, Cd, U) pH=7.00, but with a much smaller impact compared to the same conditions where the filter filling was apatite. Zeolite as an adsorbent in the column had a greater influence on the filtrates when the initial contaminated solution with toxic metals (Pb, Zn, Cd, U) was acidic, pH = 5.00. Solutions with Pb (7.31-7.23-7.22-7.18-7.15) and Zn (7.60-7.25-7.02-7.00-6.99) had sudden changes in the filtrate passed through the zeolites and a trend of decreasing pH value

with time (t1-t5). Graph 2 clearly shows that the change in the pH value of the basic contaminated solution (pH =5.00, pH =7.00) did not significantly affect the change in the pH value of the filtrate obtained through apatites for U and Pb contaminants.

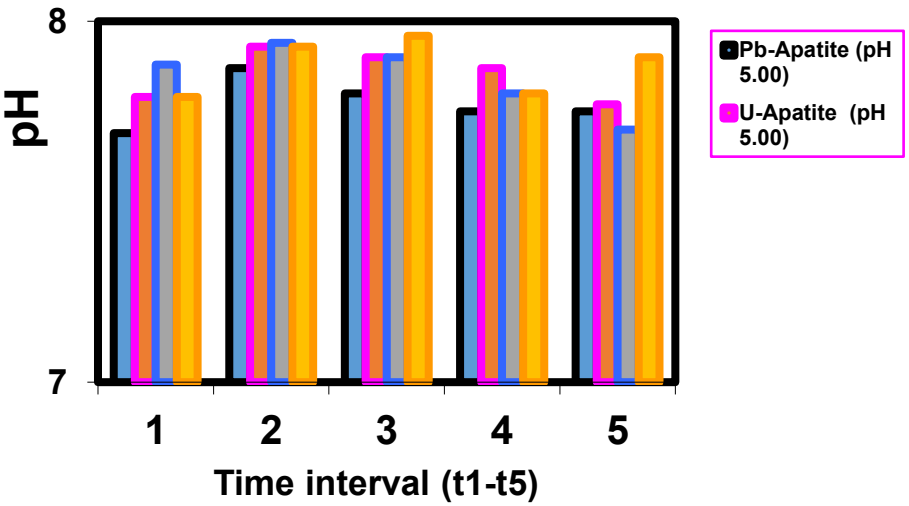

Graph. 3 The influence of the pH value of the basic contaminated solution, pH 5.00 and 7.00, on the changes in the pH value of the filtrate through apatite columns for U and Pb

The increase in the pH value of the solution during the adsorption process of Pb, Cu, Ni, Co, Zn on zeolites indicates that the zeolite is subjected to ion exchange mechanisms with the introduction of toxic metals and that the maximum level of exchange follows the order Pb^{2+} (2530 mmol g-1) > Cu^{2+} (2081 mmol g-1) > Ni^{2+} (1532 mmol g-1) > Co^{2+} (1242 mmol g1) > Zn^{2+} (1154 mmol g-1) (Qui, 2009).

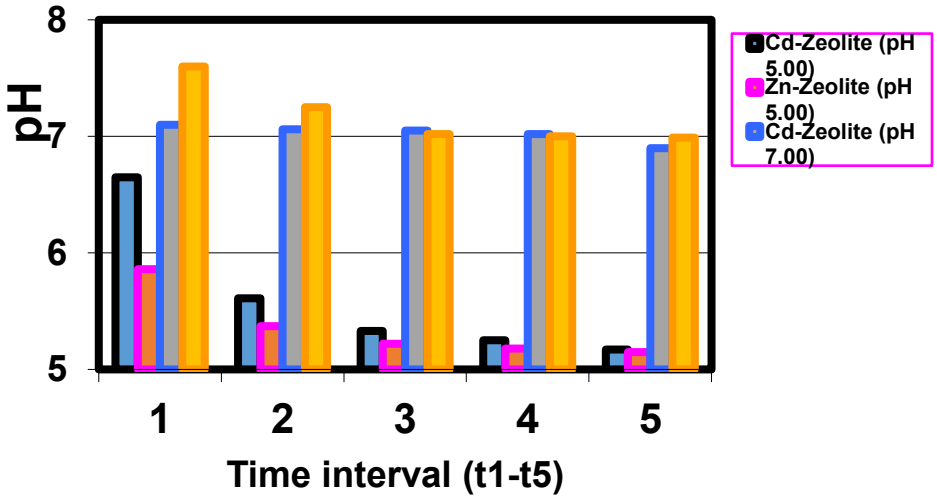

Graph. 4 The influence of the pH value of the basic contaminated solution, pH 5.00 and 7.00, on changes in the pH value of the filtrate through the zeolite columns for Cd and Zn

3 CONCLUSION

By measuring changes in the pH value of the solution, the cyclic process of zeolite saturation can be very successfully monitored, which can successfully indicate the point of saturation and the end of the regeneration process, which is very important for practical application. The column experiment showed that the best efficiency is obtained if the initial lead concentration is 1,026 mmol l^{-1} and the flow rate is 2 ml $min.^{-1}$ (Vukojevic, 2006).

The filtrate obtained from the column with zeolite for the basic contaminated solutions of Cd and Zn strongly depends on the pH value of the basic solution, such differences, the dependence of Zn and Cd on the pH of the environment in which they are found, indicates that the adsorption properties of the zeolite towards Cd and Zn will depend a lot on pH of the environment (graph 4).

ACKNOWLEDGMENTS

This work was financially supported by the Ministry of Education, Science and Technological Development of the Republic of Serbia (Grant Nos. 451-03-47/2023-01/200023).

REFERENCES

JAIN C.K., RAM D. (1997) Adsorption of lead and zinc on bed sediments of river Kali. Water Research, Vol. 31, No 1: 154 –162.

KNOX A. S., KAPLAN D. I., ADRIANO D.C. AND HINTON T.G. (2003) Evaluation of Rock Phosphate and Phillipsite as Sequestering Agents for Metals and Radionuclides. Journal of Environmental Quality, Vol. 32: 515-525.

CONCA J. L. (1997) Phosphate-Induced Metal Stabilization (PIMS). Final Report to the U. S. Environmental Protection Agency #68D60023, Res. Triangle Park, NC

MATUSIK J., BAJDA T., MANECKI M. (2012) Aqueous cadmium removal by hydroxylapatite and fluoroapatite. Geology, Geophysics & Environment, Vol. 38, No. 4, 427–438.

MANECKI M., MAURICE P.A., TRAINA S.J. (2000) Kinetics of aqueous Pb+2 reaction with apatites. Soil Science, Vol. 165: 920-942.

QIU W., ZHENG Y. (2009) Removal of lead, copper, nickel, cobalt, and zinc from water by a cancrinite-type zeolite synthetized from fly ash. Chemical Engineering Journal, Vol.145: 483-488.

VUKOJEVIC-MEDVIDOVIC N., PERIC J., TRGO M. (2006) Column performance in lead removal from aqueous solutions by fixed bed of natural zeolite–clinoptilolite. Separation and Purification Technology, Vol. 49: 237–244.

УНИВЕРЗИТЕТ У БЕОГРАДУ
РУДАРСКО-ГЕОЛОШКИ ФАКУЛТЕТ
11120 Београд 35, Ђушина 7, п.п. 35-62
Тел: (011) 3219-100, Факс: (011) 3235-539

UNIVERSITY OF BELGRADE,
FACULTY OF MINING AND GEOLOGY
Republic of Serbia, Belgrade, Djusina 7
Phone:(381 11) 3219-100, Fax:(381 11) 3235-539

РУДАРСКИ ОДСЕК

Студијски програм
РУДАРСКО ИНЖЕЊЕРСТВО

Модули:

Површинска експолатација лежишта минералних сировина
Подземна експолатација лежишта минералних сировина
Подземна градња
Рударска мерења
Механизација у рударству
Припрема минералних сировина

Студијски програм
ИНЖЕЊЕРСТВО НАФТЕ И ГАСА

Студијски програм
ИНЖЕЊЕРСТВО ЗАШТИТЕ ЖИВОТНЕ СРЕДИНЕ

Деканат

- Тел.: +381 11 3219 101
- Факс.: +381 11 3235 539
- E-mail: dekan@rgf.bg.ac.rs

Рударски одсек

- Секретар: Томашевић Александра
- Тел.: +381 11 3219 102
- E-mail: ro@rgf.bg.ac.rs

Секретар факултета

- Ђокановић Слађана
- Тел.: +381 11 3219 105
- E-mail: sladja@rgf.bg.ac.rs

Геолошки одсек

- Секретар: Јевтовић Бошко
- Тел.: +381 11 3219 103
- E-mail: gorgf@rgf.bg.ac.rs